

Investigating calcium signalling in *Marchantia polymorpha*: A study of CBLs and CIPKs.

James Houghton

February 28th 2024

This thesis is submitted for the qualification of Master of Science by Research at the University of East Anglia, research conducted in the School of Biology.

This copy of the thesis has been supplied on condition that anyone who consults it is understood to recognise that its copyright rests with the author and that use of any information derived therefrom must be in accordance with current UK Copyright Law. In addition, any quotation or extract must include full attribution

Abstract

Global food security is one of the preeminent challenges facing the modern world as a rising population demands an ever increasing volume of food to feed it. However, simultaneously climate change through both drought and other extreme weather events is proceeding to destroy arable land, leaving less and less viable farming space every year. In order to help combat this, generations of more hardy crop plants could be generated to use this otherwise unusable land. But in order to do this we need to understand better just how plants respond to the stresses currently rendering the land useless.

Calcium is a ubiquitous secondary messenger in plants which is involved in a variety of stress responses including physical, biotic and abiotic stresses by creating calcium signals. Plants decode these signals through a suite of decoder proteins, however years of evolution and hybridisation events have left the genome of crop plants highly convoluted and difficult to decipher. However, *Marchantia polymorpha* is one of the earliest diverging land plants, with a much reduced set of decoder proteins, making it an excellent tool for studying both how these stress responses evolved, and how the systems themselves operate.

This work investigates a particular subset of these decoder proteins, Calcineurin B-Like proteins (CBLs) and their interacting partners, CBL-Interacting Protein Kinases (CIPKs). When compared to the tradition plant model organism *Arabidopsis thaliana* I have shown that both CIPKs of *M. polymorpha* bind CBLs non-specifically, binding to all three native CBLs as well as AtCBL4 from *Arabidopsis thaliana*. This total promiscuity is not shared by AtCIPK24, failing to bind CBL-C from *M. polymorpha*. Additionally, work has begun on identifying the stresses that CIPKs are responsible for, a phenotyping experiment utilising *cipk-B* KO mutants showing that CIPK-B is necessary for salt tolerance in *M. polymorpha*.

Access Condition and Agreement

Each deposit in UEA Digital Repository is protected by copyright and other intellectual property rights, and duplication or sale of all or part of any of the Data Collections is not permitted, except that material may be duplicated by you for your research use or for educational purposes in electronic or print form. You must obtain permission from the copyright holder, usually the author, for any other use. Exceptions only apply where a deposit may be explicitly provided under a stated licence, such as a Creative Commons licence or Open Government licence.

Electronic or print copies may not be offered, whether for sale or otherwise to anyone, unless explicitly stated under a Creative Commons or Open Government license. Unauthorised reproduction, editing or reformatting for resale purposes is explicitly prohibited (except where approved by the copyright holder themselves) and UEA reserves the right to take immediate 'take down' action on behalf of the copyright and/or rights holder if this Access condition of the UEA Digital Repository is breached. Any material in this database has been supplied on the understanding that it is copyright material and that no quotation from the material may be published without proper acknowledgement.

Contents

1	Introduction	
1.1	Calcium signalling in plants	5
1.1.1	Calcium signals are encoded by release of Ca ²⁺ ions into the cell.	5
1.1.2	Calcium signals are decoded by a wide variety of decoder proteins	6
1.2	Overview of CBL/CIPK structure and function	7
1.2.1	Structure/function of EF hands	7
1.2.2	Structure/function of NAF domain	8
1.2.3	Structure/function of kinase domain	10
1.2.4	Structure/function of PPI domain	10
1.2.5	SOS as a model for the CBL-CIPK network	11
1.3	<i>Marchantia polymorpha</i> as a model organism	12
1.3.1	An overview of the role of <i>Marchantia polymorpha</i> in research	12
1.3.2	Why use <i>Marchantia polymorpha</i> for the study of CBLs and CIPKs?	12
2	Materials and Methods	
2.1	Materials and Methods	14
2.1.1	Cloning Methods and <i>in vitro</i> validation	14
2.1.2	NanoBiT assays and preparations	16
2.1.3	Working with <i>Marchantia polymorpha</i>	18
3	Results and discussions	
3.1	Introduction	20
3.1.1	Understanding calcium signalling in <i>Marchantia polymorpha</i> is a route to more resilient plants	20
3.1.2	An overview of the main technologies used	21

3.1.3	Previous work and the next steps	23
3.2	Identifying CBL-CIPK interactions in <i>M. polymorpha</i>	25
3.2.1	Cloning: Level 0 to Level 2	25
3.2.2	NanoBiT assay indicates there is no specificity in CBL-CIPK interactions in <i>Marchantia polymorpha</i>	33
3.3	CIPK-B is necessary for salt tolerance in <i>Marchantia polymorpha</i>	35
4	Conclusion	39
A	Appendix	40
B	Bibliography	41

Chapter 1

Introduction

1.1 Calcium signalling in plants

1.1.1 Calcium signals are encoded by release of Ca^{2+} ions into the cell.

Plants and other eukaryotes use calcium (Ca^{2+}) as a ubiquitous secondary messenger in a process known as Calcium Signalling (Berridge, Lipp and Bootman, 2000). The range of stimuli which trigger a calcium signalling response includes both biotic and abiotic stresses. Biotic responses include pathogen responses (Nhieu et al., 2004) and symbiosis events, as seen in the nodulation of legumes by *Rhizobia* (Ehrhardt, Wais and Long, 1996). Abiotic responses include physical stresses such as touch (Braam et al., 1996) and light (Bush, 1995), ionic stresses like high salinity (Knight, Trewavas and Knight, 1997) or potassium starvation (Xu et al., 2006), as well as osmotic stresses such as drought (Staxén et al., 1999). When introduced to a stress, a calcium signalling response is triggered producing a unique Ca^{2+} signature. During a Ca^{2+} signature the concentration of intracellular cytosolic Ca^{2+} is raised from the basal level of between 100-200 nM, via either the influx of extracellular Ca^{2+} which is maintained at mM concentrations or the mobilisation of intracellular stores of Ca^{2+} . The influx of Ca^{2+} ions is rapidly extruded from the cell against the concentration gradient via ion channels. Measuring the concentration of Ca^{2+} in the cell over a time period generates a graph as depicted below in Fig.1.1. The amplitude of the signal is determined by the amount of Ca^{2+} released into the cell. Some Ca^{2+} signatures involve repeated influx and efflux of Ca^{2+} , measuring the time between these events provides a frequency.

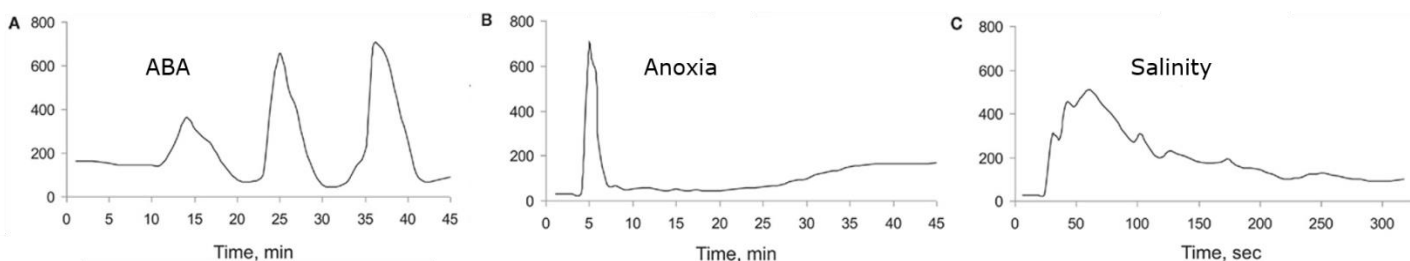


Fig.1.1 Example measurements of Ca^{2+} signature response to a range of stimuli. A: Response to 10 nM ABA treatment (Staxén et al., 1999); **B:** response to anoxia (Sedbrook et al., 1996); and **C:** response to salt (Tracy et al., 2008)

As can be seen in Fig.1.1 the amplitude, duration, and frequency of the responses differ in each condition. Response to the stress hormone abscisic acid (ABA) elicits an oscillation of cytosolic Ca^{2+} in spikes that last approximately five minutes, every five minutes (Staxén et al., 1999). Anoxia response initially generates a single sharp peak, lasting only a couple of minutes before a gradual build-up of Ca^{2+} at a relatively low level which lasts for hours (Sedbrook et al., 1996). The salinity response produces just a single peak in a response which lasts around five minutes (Tracy et al., 2008).

1.1.2 Calcium signals are decoded by a wide variety of decoder proteins.

In order to properly respond to these highly variable Ca^{2+} signatures, and bring about the correct physiological responses, these signals are decoded and 'read' by a suite of so-called decoder proteins. A selection of which can be seen in Fig.1.2

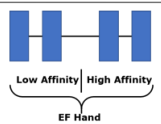
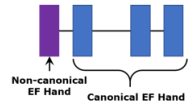
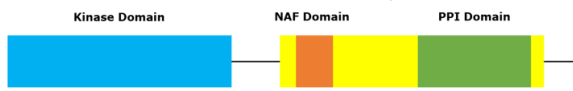

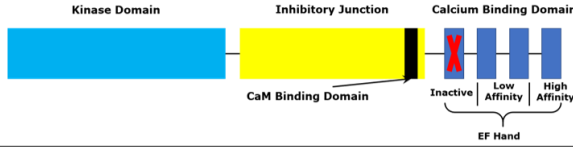

Name	Domain Structure	Count in <i>A. thaliana</i>
Calmodulin (CaM)		7
Calcineurin B-like Protein (CBL)		10
CBL Interacting Protein Kinase (CIPK)		26
Calmodulin Dependent Protein Kinase (CaMK)		4
Calcium and Calmodulin Dependent Protein Kinase (CCaMK)		0 (Animal only)
Calcium Dependent Protein Kinase (CDPK)		34

Fig.2.1 A schematic of the important domains of a range of calcium sensors and their interacting kinases. CaMs and CBLs are both capable of sensing calcium via EF hand domain. CCaMKs and CDPKs are also capable of sensing Ca^{2+} via EF hands. The kinases all contain an intrinsic kinase domain, as well as a regulatory domain known as the inhibitory junction. Both CaMK and CCaMK possess CaM binding domains in this inhibitory junction. CIPKs possess a NAF domain, required for interaction with CBLs and a protein-phosphate interaction (PPI) domain. A count of the number of known proteins in each group in *Arabidopsis thaliana* has also been provided.

Calcium Dependent Protein Kinases (CDPKs) are capable of both sensing Ca^{2+} and phosphorylating downstream targets, such as ion channels and transcription factors to regulate their activity. This allows them to work independently as a Ca^{2+} decoder. (Cheng, Willmann, Chen and Sheen, 2002) Other decoder proteins are not capable of this feat and require an interacting partner, forming a two component system. Calmodulin Dependent Protein Kinases (CaMKs) use Calmodulin (CaM), a small Ca^{2+} sensor protein, to react to Ca^{2+} fluctuations. (Wayman et al., 2011) Similarly, Calcium and Calmodulin Dependent Protein Kinases (CCaMKs), only found in animals, utilise CaM to sense Ca^{2+} . However, they also possess the ability to natively sense Ca^{2+} , though the presence of CaM is required to activate the protein. Whereas CaM is highly promiscuous, capable of binding to many different proteins types, the Ca^{2+} sensors Calcineurin B-like proteins (CBLs) are much more specific. They are only capable of binding with CBL-interacting protein kinases (CIPKs), and indeed, not all CBLs are capable of binding with all CIPKs. While there are examples of both CBLs capable of binding to multiple different CIPKs and the inverse, there is still a high level of selection between CBL-CIPK interactions in flowering plants (Kolukisaoglu *et al.*, 2004)

The most important domain across the calcium decoder proteins is the EF hand domain, as it is this domain which binds Ca^{2+} . The EF hands of CaMs and CBLs function in pairs, with each EF hand being capable of coordinating a single Ca^{2+} ion. (Nelson et al., 2009) The affinity of each EF hand, and thus each pair, is different leading to varied Ca^{2+} affinities for each Ca^{2+} sensor. This enables the selectivity of the sensors to their Ca^{2+} signatures.

1.2 Overview of CBL/CIPK structure & function

1.2.1 Structure/function of EF hands

EF-hands are calcium binding domains found in the calcium sensor proteins CaMs and CBLs, as well as the kinases CDPKs and CCaMKs. It is these domains which enable these proteins to detect changes in calcium concentration. The overall structure of the EF hand follows a helix-loop-helix motif (Fig.1.3.A), where calcium is coordinated in the loop section (Sanchez-Barrena et al., 2013). Through the majority of calcium sensing proteins, the EF-hand motif is highly conserved, following a 12 amino acid consensus sequence DxDxDGKxDxxE (Kolukisaoglu *et al.*, 2004; Li *et al.*, 2009). Positions 1 (X), 3 (Y), 5(Z), 7 (-Y), 9 (-X) and 12 (-Z) of the loop are responsible for calcium coordination. In canonical EF-hands, calcium is coordinated in a pentagonal-bipyramidal manner, using side chain donor oxygen at positions X, Y, Z and -Z; main chain carbonyl oxygen at -Y; and is mediated by a water molecule at -X. However, when looking at the EF hands of CBLs in Arabidopsis, it has been

found that the vast majority are non-canonical. For instance, the first EF-hand (EF1) exhibits an extended loop domain with a two amino acid insertion between positions X and Y. Additionally, in most of the CBL EF-hands there is a D>K substitution at position Y. One would expect such a mutation at a critical residue would impair the calcium binding function, however this does not appear to be the case. Calcium is still coordinated at this position, now using the main chain carbonyl as at position -Y (Fig.1.3B).

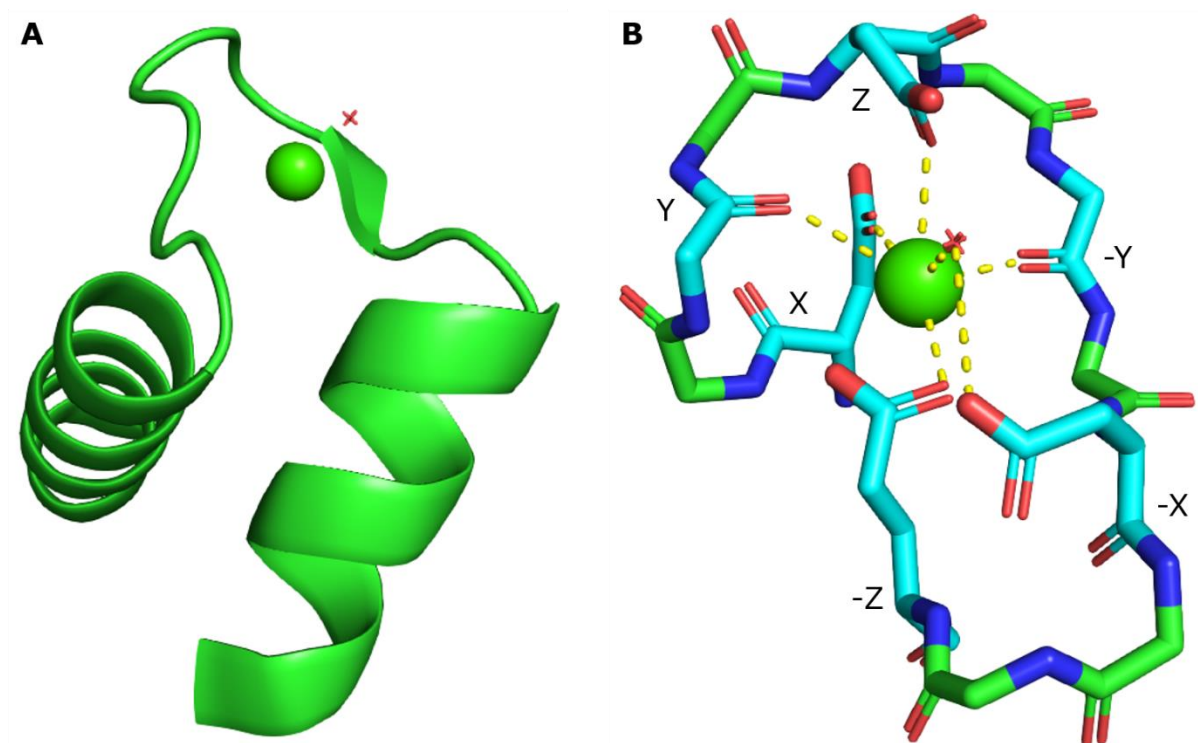


Figure.1.3 Crystal structure of AtCBL-4 EF4. **A:** Overall helix-loop-helix EF-hand structure, with bound calcium depicted as a green ball. (PDB code 1V1G) (Sánchez-Barrena et al., 2005) **B:** The calcium binding loop of AtCBL-4 EF4. Amino acids involved in Calcium coordination are coloured cyan and labelled accordingly. Oxygen involved in coordination has been linked to the bound calcium (green ball) with dashed yellow lines. Additionally the interaction between the water molecule and position -X is depicted with a dashed yellow line. (PDB code 1V1G)

1.2.2 Structure/function of NAF domain

First identified in 2002, the NAF domain, so called for the highly conserved NAF sequenced contained within, is both required and sufficient for the binding of CBLs and CIPKs (Albrecht et al., 2002). Found in the middle of the CIPK, the domain itself is 24 amino-acids long, made up of four discreet 6 amino-acid motifs, alternating unstructured loop and helix motifs (Sanchez-Barrena et al., 2007). Alignment of the NAF domains of AtCIPKs has shown that the first unstructured loop is highly variable, containing amino acids of various charges

and polarities at positions 1, 2, 4 and 5, while positions 3 and 6 contain mainly non-polar molecules (Fig.1.4). This motif exhibits the least conservation so is unlikely to play an important role in the binding interaction. The first helix contains the motif for which the domain is named, the highly conserved NAF sequence with the consensus sequence of NAF(D/E)(L/I)I. The amino acids at positions 8, 9 and 12 have been identified as buried in the interaction with binding CBLs (Sanchez-Barrena et al., 2007). The second unstructured loop domain is serine rich, though generally exhibits less conservation than the two helix domains. Amino acids at positions 15, 17 and 18 are buried in the CBL interaction. The final helix is less well conserved than the first, but the buried amino acids at positions 20, 23 and 24 are well conserved. Approximately half of the AtCIPKs have the same final helix of DLSGLF, or only differ by one amino acid. This is illustrated below in Fig.1.4

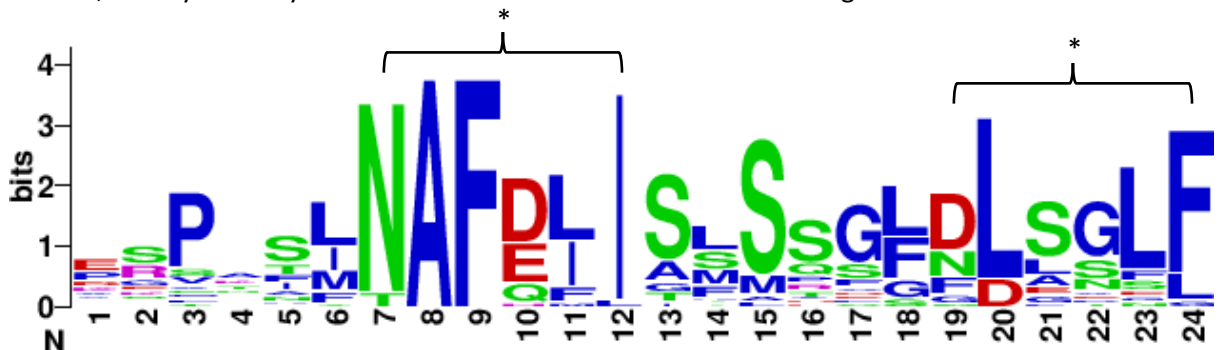


Figure.1.4 WebLOGO alignment of all atCIPK NAF domains. Amino acids are represented by their one letter code, and coloured according to their side chain type: Red for acidic, Magenta for basic, Blue for non-polar, Green for Polar non-charged. Regions marked with '*' are the two helical domains.

In order to bind with its partner CBL, the NAF domain is inserted into the binding cleft of its partner CBL. This cleft is found between the two EF-hand pairs. This binding interaction is supported by numerous hydrophobic interactions (Sanchez-Barrena et al., 2013). The mechanism for the specificity of CBL-CIPK interactions is as yet unknown. It has been postulated that the second unstructured loop domain may play a part in specificity, however this has not yet been proven *in vivo*. Additionally, while not important for the binding itself, the overall topology of both interacting proteins could be important for interaction viability, and as such simply exchanging the NAF domain between CIPKs may not be enough to change the binding specificity to another CBL (Sanchez-Barrena et al., 2013).. As an example of this, a computational model, attempting to show theoretical binding between AtCIPK24 and AtCBL2 showed that the NAF domain would overlap the EF hands of the CBL and as such could not bind at all (Sanchez-Barrena et al., 2013). Additionally, the NAF domain does not only have a role in CBL binding. It can also act as an

autoinhibitory domain, preventing activation of the kinase domain while unbound by its CBL partner by blocking the active site of the kinase domain.

1.2.3 Structure/function of Kinase domain

The kinase domains of CIPKs exhibit the canonical Serine/Threonine fold, allowing them to phosphorylate the hydroxyl groups of the aforementioned amino acids. This domain folds into two separate lobes, the N and C lobes, connected by the activation loop. The N-lobe is the smaller of the two lobes, consisting of six anti-parallel β -sheets and two α -helices, whereas the larger C lobe is mainly helical. (Chaves-Sanjuan et al., 2014) All of the residues involved in the binding of ATP, and substrates are located in the cleft between the N and C lobes. This cleft is considered the active site of the kinase and can be autoinhibited in two ways, via the activation loop, and via the NAF domain.

Both of these motifs function similarly, blocking the access of substrates to the active site, leaving the kinase domain in an 'open' inactive state. As a general model, the activation loop is controlled by the phosphorylation of three conserved residues one each of serine, threonine, and tyrosine. Phosphorylation of these residues leads to the retreat of the activation loop, moving the kinase domain towards its 'closed' active state. AtCIPK24/8 harbour a mutation which abolishes the second α -turn of the activation loop, this has a comparable effect to phosphorylation of the activation loop on kinase activity, resulting in a level of basal activity (Chaves-Sanjuan et al., 2014).

At the open inactive state, the NAF domain binds to the interface between the N and C lobes, blocking access to both the active site and the ATP binding motif. By preventing the binding of ATP and the substrate the requisite conformational changes cannot take place rendering the kinase domain inactive. (Chaves-Sanjuan et al., 2014) The binding of the partner CBL sequesters the NAF domain, leaving the kinase domain free to bind ATP and substrates and adopt the closed active state.

1.2.4 Structure/function of PPI domain

The PPI domain adopts an α/β domain, consisting of two α helices packed against a five-stranded antiparallel β -sheet of strand order $\beta 1-\beta 5-\beta 4-\beta 3-\beta 2$. The first helix ($\alpha 1$) connects $\beta 1$ and $\beta 2$, while the second helix ($\alpha 2$) comes after $\beta 5$ at the C terminal end of the domain. Critically, the protein-phosphate binding sequence (PPI motif) spans $\beta 1$ and $\alpha 1$ at the N terminus of the domain. (Mao et al., 2016) It is this sequence which is involved in the

binding of the protein phosphatases involved in the phosphorylation of the activation loop of the kinase domain, allowing for the activation of the CIPK. The PPI domain is also involved in the binding of CBLs to the NAF domain. Residues in $\beta 1$, $\beta 4$ and $\beta 5$ are involved in this binding, including residues in the PPI motif. (Mao et al., 2016) Mutation to key residues in the PPI motif has been shown to hinder the interaction of CIPKs with both partner CBLs and protein phosphatases. Direct competition experiments have shown that CIPKs are only capable of binding their CBL partners when not interacting with a protein phosphatase (Mao et al., 2016).

1.2.5 SOS as a model for the CBL-CIPK network

The most widely accepted mechanism of action for CBL-CIPK interaction is that CBLs bind Ca^{2+} released in a Ca^{2+} signature, allowing them to interact with their CIPK partner, leading to the *trans*-phosphorylation of the downstream target (Bender, Zielinski and Huber, 2018). The best characterised example of this is the forefather of CBL-CIPK signalling in the Salt-Overly-Sensitive (SOS) pathway in *Arabidopsis thaliana*. A three component system, the activity of the Na^+/H^+ antiporter SOS1 (Qui et al., 2002) is regulated by SOS3 (AtCBL4) (Ishitani et al., 2000) and SOS2 (AtCIPK24) (Liu and Zhu 1998). During a salt induced calcium signal, Ca^{2+} binds to the EF hands of AtCBL-4, which itself becomes bound to AtCIPK24 via interaction with the NAF domain. This AtCBL4/AtCIPK24 complex then activates SOS1 via a *trans*-phosphorylation reaction, enabling for control of the levels of Na^+ in the cell (Shi et al., 2002). This pathway is illustrated bellow in Fig.1.5.

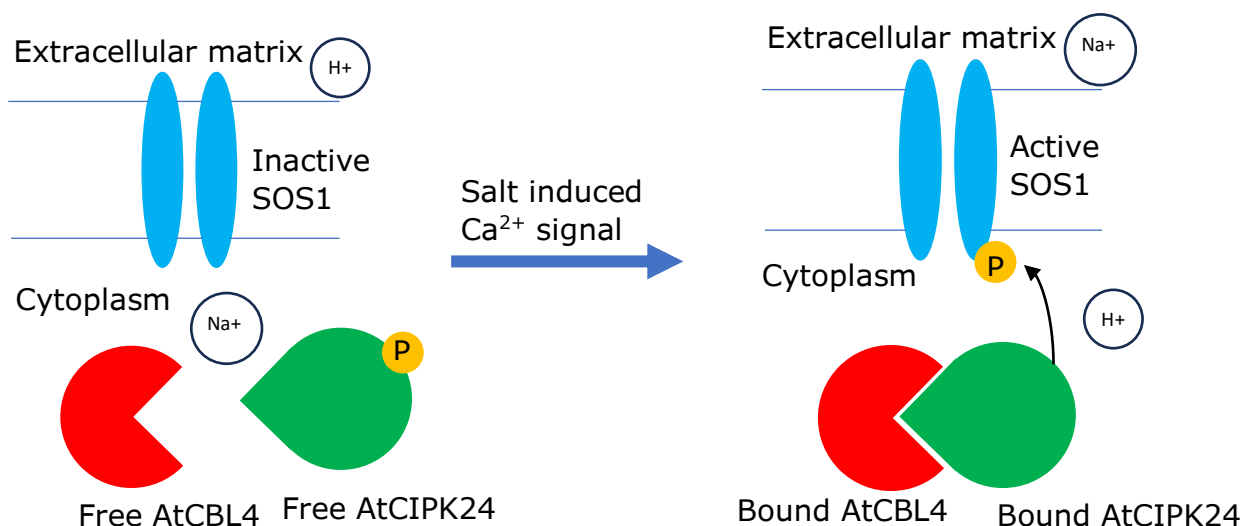


Figure.1.5 – A schematic of the action of activation of SOS1 by AtCIPK24 and AtCBL4. SOS1 is activated by *trans*-phosphorylation by the AtCBL4–AtCIPK24 complex after a salt induced Ca^{2+} signal is received, leading to exchange of H^+ and Na^+ ions.

1.3 *Marchantia polymorpha* as a model organism

1.3.1 An overview of *Marchantia polymorpha*'s role in research.

Marchantia polymorpha is a simple liverwort, evolutionarily important as one of the earliest diverging land plants. As a cousin of many of the later diverging angiosperms, the findings made in the study of the fundamental mechanisms and principles of *M. polymorpha* are applicable to a wide range of other plants. One of the benefits of using *M. polymorpha* as a model organism is the ease with which it can be cultivated. As a dioecious plant, *M. polymorpha* is capable of sexual reproduction. However it is also capable of asexual reproduction through the production of gemmae – clonal propagules with two apical meristems, as well as from cuttings of thallus tissue. This variety of different reproduction methods allows for easy genetic analyses and maintenance of plant lines. Additionally, it is fast growing, growing from a single gemmae to a gemmae producing plant in just three weeks. Another benefit of working with *M. polymorpha* is its simple haploid genome of 280 Mb. This genome has been sequenced and is a good resource for the identification of genes of interest (Bowman *et al.*, 2017). Moreover, *M. polymorpha* is amenable to transformation by *Agrobacterium tumefaciens*, allowing for the knockout of genes using CRISPR technology.

1.3.2 Why use *Marchantia polymorpha* for the study of CBLs and CIPKs?

Much of the research into Ca²⁺ signalling in plants has been carried out using *Arabidopsis thaliana*, as the model. However, one problem that studies using *A. thaliana* run into is the vast array of CBLs (10) and CIPKs (26) in this species (Edel & Kudla, 2015). Many of these are functionally redundant so it is difficult to determine the exact functions of each protein (Kudla *et al.*, 1999). *M. polymorpha*, on the other hand, has just 3 CBLs, CBL-A, CBL-B and CBL-C and 2 CIPKs, CIPK-A and CIPK-B (Edel & Kudla, 2015)(Tansley *et al.*, 2022), far fewer than *A. thaliana*. This leaves just six possible combinations of CBLs and CIPKs, compared to the theoretical 260 combinations available in *A. thaliana*. This makes the CBL-CIPK network much easier to unpick in *M. polymorpha*, reducing the likelihood of issues with functional redundancy. Bioinformatics work in the Miller lab has shown that the CBLs and CIPKs in *M. polymorpha* are related to a range of CBLs and CIPKs in *A. thaliana*, see Fig.1.6 (Tansley, Unpublished).

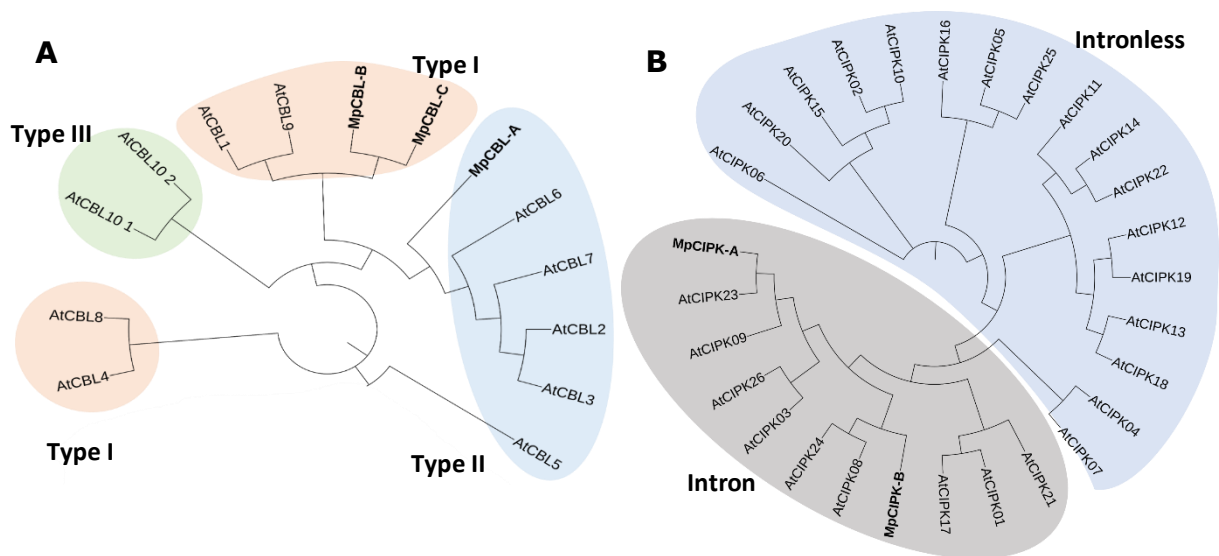


Figure.1.6 Phylogeny trees comparing the CBLs and CIPKs of *M. polymorpha* and *A. thaliana*. A) Phylogeny of MpCBLs (Bold) and AtCBLs, shading represents CBL putative localisation types, type I in orange, type II in blue and type III in green (Edel & Kudla, 2015). B) Phylogeny of MpCIPKs (bold) and AtCIPKs, shading represents CIPK types, those with Introns, and those without (Edel & Kudla, 2015). (Images provided by Dr Connor Tansley, Unpublished).

Work has started on identifying the interactions between MpCBLs and MpCIPKs, first using yeast-two-hybrid assays. This has identified a range of interactions (Tansley *et al.*, 2022) and my work has been first focused on confirming these interactions *in planta* using *Nicotiana benthamiana* as a heterologous host. Additionally, stress phenotyping using qPCR has shown that the expression of *MpCIPK-B* is affected by salt concentrations (Tansley *et al.*, 2022), leading to the hypothesis that it could be the *SOS2* homologue. Following this, two knockouts of *MpCIPK-B* in *M. polymorpha* have been generated in the Miller Lab, using CRISPR/Cas9 gene editing, by Dr Connor Tansley, and characterised by Althea Rose (Tansley *et al.*, 2022).

Chapter 2

Materials and Methods

2.1 Materials and Methods

2.1.1 Cloning methods and *in vitro* validation

Sub-cloning AtCLB4 to SC position in the golden gate cloning model

Synthetic cDNA of AtCBL4 was amplified using the primer pair c222/c223 (Appendix.1). These primers add *Bsa*I restriction sites flanking the gene, as well as the downstream fusion sites, AATG and GCTT that the type IIS restriction enzyme will cleave, allowing for the modular and directional nature of golden gate cloning (Weber *et al.*, 2011). The PCR was carried out in a single tube, 20 μ l reaction containing: 100 ng of template, 8 μ M of each primer, 4 mM dNTPs (Thermo Fisher Scientific), 1x HF buffer (Thermo Fisher Scientific), 0.4 U Phusion DNA Polymerase (Thermo Fisher Scientific) and an appropriate amount of water to bring the reaction to 20 μ l. The reaction was incubated in a thermocycler following the programme seen in Table.2.1.

Table.2.1 Thermocycler programme for Phusion PCR

Number of cycles	Temperature (°C)	Time (s)
1	98	30
30	98	10
	53	20
	72	90
1	72	300
Hold	10	-

Gel electrophoresis

4 μ l of 6x Loading Dye (NEB) was added to each sample unless GoTaq (Promega) had been used for the PCR. Each sample was loaded onto a 1% agarose gel (Sigma) alongside a 1kb+ ladder (NEB), and ran at 120 V for 25 minutes. Gels were post-stained in a 0.5 μ g/mL Ethidium bromide (Sigma) solution for 10 min and then visualised using a FLA9500 Typhoon scanner.

Gel extraction

The required DNA fragments were extracted from agarose gels using the QIAquick Gel Extraction Kit as per manufactures instruction (Qiagen). DNA was eluted in 20 µl of water.

Golden Gate Assembly

Golden Gate Assembly was carried out over Levels 0, 1 and 2 following the same framework - a single tube 15 µl reaction comprised of: 100 ng of each insert as per Appendix.2,3,4, 1x BSA (NEB), 1x T4 DNA Ligase Reaction Buffer (NEB), 400 U T4 DNA Ligase (NEB), 5 U Type IIS restriction enzyme, and an appropriate amount of water to bring the reaction to 15 µl. Levels 0 and 2 use *Bpil* (Thermo Fisher Scientific), Level 1 uses *Bsal* (Thermo Fisher Scientific) as the Type IIS restriction enzymes. The reaction was incubated in a thermocycler following the programme seen in Table.2.2.

Table.2.2 Thermocycler programme for Golden Gate Assembly

Number of cycles	Temperature (°C)	Time (min)
25	37	3
	16	4
1	50	5
	80	5
Hold	10	-

E.coli transformation

1 µl of each Golden Gate product was incubated with 20 µl of competent *Escherichia coli* DH5α cells (Level 0, Level 1) or DH10B (Level 2) on ice for 20 minutes, followed by a 30 second heat shock at 42°C. The cells were immediately placed on ice for a minimum of 2 minutes before 500 µl of SOC media (Formedium) was added. Following this, the cells were incubated at 37°C, shaking in a ThermoMixer at 300 rpm for 1 hour. Once incubation was complete 200 µl of the cell suspension was plated on to LB-agar plates (Sigma). Level 0 plates contain 100 µg/ml Isopropyl β- d-1-thiogalactopyranoside (IPTG) (Thermo Fisher Scientific), 40 µg/ml 5-bromo-4-chloro-3-indolyl-β-D-galactopyranoside (X-gal) (Sigma) and 100 µg/ml spectinomycin (Sigma). Level 1 plates contain 100 µg/ml IPTG (Thermo Fisher Scientific), 40 µg/ml X-gal (Sigma) and 100 µg/ml ampicillin (Thermo Fisher Scientific). Level 2 plates contain 25 µg/ml Kanamycin (Sigma). The plates were incubated at 37°C overnight.

Colony PCR

White colonies were selected and added to a 10 µl reaction containing: 5 µl 1x GoTaq Master Mix (Promega), 20 µM of each primer (See Appendix.1) and an appropriate amount of water to bring the reaction to 10 µl. The reaction was incubated in a thermocycler following the programme seen in Table.2.3. Agarose gel electrophoresis as then performed as above.

Table.2.3 Thermocycler programme for colony PCR.

Number of cycles	Temperature (°C)	Time (s)
1	98 °C	600
30	98 °C	10
	53 °C	20
	72 °C	60 / kb
1	72 °C	300
Hold	10 °C	-

E. coli culture

Colonies identified as positive through colony PCR were grown up overnight in 5 mL LB broth (Formedium) containing appropriate antibiotics. Plasmid DNA was extracted from *E. coli* cultures using the Wizard Plus SV Minipreps DNA Purification System as per the manufacturer's instructions (Promega). DNA quality and concentration was assessed using a NanoDrop spectrophotometer (Thermo Fisher Scientific). 10 µl of Isolated DNA was added to a sequencing tube alongside 2 µl of primer and 7 µl of water and Sanger sequenced by Eurofins genomics. The returned data was analysed using the NCBI BLAST software, comparing the sequencing data to a reference plasmid map generated in ApE.

2.1.2 NanoBiT assays and preparations.

Agrobacterium transformations

1 µl of DNA of each Level 2 construct (appendix.2C) was added to 20 µl of GV3101 A. *tumefaciens* competent cells and immediately flash-frozen in liquid nitrogen. The samples were then thawed at 37 °C for 1 minute. Next 500 µl of SOC media was added, before incubating the samples at 28 °C, shaking in a ThermoMixer at 300 rpm for 2 hours. Once incubation was complete 200 µl of the cell suspension was plated on to LB-agar plates

(Sigma) containing 50 µg/ml rifampicin (Thermo Fisher Scientific), 80 µg/ml gentamycin (Sigma) and 50 µg/ml kanamycin (Sigma). The plates were incubated at 28 °C for 3 days.

***Agrobacterium* culture**

Colonies identified as positive through colony PCR (as above) were grown in LB broth (Formedium) containing 50 µg/ml rifampicin, (Thermo Fisher Scientific), 80 µg/ml gentamycin (Sigma) and 50 µg/ml kanamycin (Sigma) overnight at 28°C, shaking at 300rpm

***Nicotiana benthamiana* transformation**

Agrobacterium overnight cultures were centrifuged at 4000 rpm for 8 minutes to produce a pellet. Each pellet was resuspended in 1 mL of 150 µM acetosyringone in water and diluted to an OD of 0.3 which was verified by a spectrophotometer. These *Agrobacterium* suspension, as well as an acetosyringone control, were infiltrated into separate leaves of 4-6 week old *N. benthamiana* plants using 1 mL needleless syringes (Medisave) and left for three days at standard room conditions.

β-glucuronidase (GUS) staining

Size 6 leaf discs were added to 1 mL of GUS staining buffer and infiltrated into the leaf discs using a vacuum desiccator. GUS staining buffer contained 0.1% Triton X-100 (Sigma), 1 mM EDTA at pH 8 (Sigma), 50 mM NaPO₄ at pH 7 and water to make up to the desired volume. Once the staining buffer had fully infiltrated the leaf, they were incubated at 37°C for 1 hour. Successful transformation was indicated by the development of blue pigment.

Protein Extraction

Protein extraction buffer was prepared fresh, containing 100 mM TRIS-HCL (pH 8.0), 5 mM EDTA (Sigma), 1.5 mM DTT (Sigma), 10% glycerol (Thermo Fisher Scientific), one cOmplete Mini EDTA-free protease inhibitor tablet (Roche) per 10 mL of buffer produced, and water to make up the desired volume of buffer. Plant material was harvested from each infiltration site, using a size 6 cork borer and placed in a 1.5 mL Eppendorf tube and flash-frozen in liquid nitrogen. Plant tissue was homogenised in 150 µl of protein extraction buffer using microcentrifuge tube pestles and then incubated on ice for at least 10 minutes. Plant material was pelleted in a microcentrifuge at 14,000 rpm for 10 minutes at 4 °C and the supernatant transferred to a clean 1.5 mL Eppendorf tube.

Nano-Glo® Live Cell Assay System Protein assay

Dilution buffer was prepared fresh and was derived from the Nano-Glo® Live Cell Assay System kit (Promega) containing substrate, the LCS dilution buffer and water in a 1:50:49 ratio. To measure luciferase activity, 20 µl of each protein sample was added to a white flat-bottomed 96-well plate (VWR) and 40 µl of the dilution buffer added to each sample. Using a Hidex sense microplate reader, luminescence readings were made in triplicate for each protein sample.

2.1.3 Working with *Marchantia polymorpha*

Growth and phenotyping of *Marchantia polymorpha*

Stock *M. polymorpha* tissue was grown from gemmae on ½ MS media (2.165g of MS, 10g of sucrose, 8g of agar in 1L of water to a final pH of 6) for between three and four weeks.

Supplemented media plates were generated as following Table.2.4. Five cuttings from the replicating tissue at the tip of the thallus were added to each plate and grown in a growth cabinet under long day conditions. Plants on the salt treatment were grown for one week, photographed, fresh weights measured, and the chlorophyll extracted and quantified.

Table.2.4 Conditions for phenotyping

Condition	[Stock]	Water Volume (µL)	Stock Volume (µL)	Media Volume (mL)
Control	-	600	-	19.4
NaCl 50 µM	5 M	400	200	19.4
NaCl 100 µM	5 M	200	400	19.4
NaCl 150 µM	5 M	0	600	19.4

Chlorophyll extraction

To assess chlorophyll content, an adapted protocol from Caesar *et al.*, (2018) was used. Plant tissue was removed from the plate, and weighed in an Eppendorf tube. To each sample first 10 µL of 200 mM NaCO₃ was added, followed by 500 µL of DMSO (Sigma). The plant tissue was then homogenised using a micro pestle and incubated at 65°C for 90 minutes. Another 500 µL of DMSO was added and the incubation repeated. The samples were then clarified by centrifugation at 5000rpm for 10 minutes. Once clear, 200 µL of each sample was added to a clear 96 well plate in triplicate and the absorbance measured at 648nm, 665nm, and 700nm. In the case the 665 absorbance being greater than 0.8, the

sample was diluted in a 1:1 ratio of DMSO to sample. Chlorophyll content was calculated following the equation:

$$((A665 - A700) * 8.02 + (A648 - A700 * 20.2) * D * S$$

Where D is the dilution factor (usually 1, raised to 2 for the first dilution, 4 for the second etc.), and S is the amount of solvent (In this case 0.2). Standard error was calculated and statistical significance calculated by way of a Dunn's test.

Chapter 3

Results and discussions

3.1 Introduction

3.1.1 Understanding calcium signalling in *Marchantia polymorpha* is a route to more resilient plants

Food security is threatened by climate change

One of the greatest challenges facing humanity in the current day is the changing climate and the challenges it brings. One of these challenges is the impact on global food security. As the climate changes, drought is becoming more prevalent (Mukherjee *et al.*, 2018), leading to reduced crop yield of between 30 and 90% in extreme cases (Hussain *et al.*, 2019). Additionally, drought can drive up the salinity of soil, destroying it for future use. It is estimated that more than 50% of currently used arable land will be salinized by 2050 (Jamil, Riaz and Foolad, 2011) and as such we need to develop methods to combat this at a time when the demand for food is only increasing with the ever-growing population of the world. One way is by developing crop plants which are more resilient to salinity. To do this however, the mechanisms of how plants respond to salt and other abiotic stimuli needs to be studied.

Plants respond to abiotic stress via calcium signalling

One of the main ways that plants respond to abiotic stresses is through calcium signalling. In response to a stress, such as salinity, a unique calcium signature is generated. To be able to respond to this signal, it is decoded by a range of so called decoder proteins. The most common example of this is the CBL-CIPK mediated Salt Overly Sensitive pathway characterised in *A. thaliana* (Shi *et al.*, 2002). However, further study of the CBL-CIPK network in *A. thaliana* is difficult due to the high counts of CBLs (10) and CIPKs (26) leading to convoluted functional redundancy (Edel & Kulda, 2015). Studying the much more reduced system of *M. polymorpha*, containing just three CBLs and two CIPKs has many benefits, including removing that complexity. Additionally, as a bryophyte *M. polymorpha* is one of the earliest land plants, studying the rise of this signalling network could produce profound insights as to how it was initially developed. It is our hope that these insights can

be leveraged to help elucidate the signalling networks in crop plants with vastly more complex genomes, and later help improve them to develop more resistant plants. In this study we hope to make that first step by characterising the interactions between the CBLs and CIPKs of *M. polymorpha* using a split-luciferase assay. Additionally we will begin to investigate the roles of these proteins in the calcium signalling network through phenotyping experiments, starting with MpCIPK-B through the use of *Mpcipk-b* mutants. The initial testing described in this work will be on salt tolerance, as MpCIPK-B has been identified as a likely homologue for the well studied AtCIPK24, both phylogenetically, and through qPCR testing (Tansley *et al.*, 2022)

3.1.2 An overview of the main technologies used

NanoBiT

To acquire an *in planta* view of the possible interactions between the CBLs and CIPKs of *M. polymorpha*, we used a novel split luciferase system known as NanoLuc® Binary Technology (NanoBiT). A split luciferase assay utilises the bioluminescent properties of a luciferase protein, commonly *Renilla* or firefly to investigate binding of proteins. The luciferase protein is split into two subunits, rendering the protein incapable of luminescence. Each half of the luciferase protein is then fused to one of the proteins of interest via cloning techniques and simultaneously expressed in a homologous system. In the case of the proteins of interest interacting, the luciferase protein will recombine, allowing it to luminesce. Similar examples exist with fluorescent proteins such as BiFC (Kerppola, 2008). NanoBiT is similar to its firefly and *Renilla* luciferase cousins in that it utilises a bioluminescent protein, NanoLuc luciferase. The specific activity of the NanoLuc luciferase is over 150 times greater than traditional *Renilla* and firefly luciferases, (Hall *et al.*, 2012) and is one of the reasons it has been chosen for this study. Another advantage it holds is its small size at just 19 kDa it is nearly half the size of *Renilla* luciferase at 36 kDa (Matthews, Hori and Cormier, 1977) and nearly a third of firefly luciferase at 62kDa (Wet *et al.*, 1985). Cleavage into its component subunits, the LargeBiT (18 kDa) and the SmallBiT (1.3 kDa), leaves two small proteins suitable for fusion tagging proteins of interest. The small size of both subunits means that there is less possibility of steric hinderance than the traditional luciferases, reducing the chance of false negative results. Additionally, the NanoBiT fragments have low affinity for one another (Dixon *et al.*, 2015), ensuring that they will only recombine when brought together by the interacting proteins. It is a combination of all these factors that informed the choice of NanoBiT for this assay.

Golden Gate Cloning

In order to generate the required fusion proteins, a DNA assembly method is required. Here MoClo (Weber et al., 2011) has been used, a technology based upon the Golden Gate system (Engler, Kandzia and Marillonnet, 2008). MoClo utilises a level system from 0 to 2 describing the complexity of the construct. Level 0 constructs contain a single element: promoters, fusion tags, genes or terminators. Level 1 constructs form a transcriptional unit containing a selection of the Level 0 elements. This transcriptional unit includes the gene of interest and the fusion tag, flanked by the promoter and terminators. CBLs were fused to the LargeBiT at the C-terminus, CIPKs were fused to the SmallBiT at the N-Terminus (Batistič *et al.*, 2009). Level 2 constructs form multigene constructs containing multiple transcriptional units, in this case tagged CBL and CIPK units, as well as a GUS module for use as an internal control. This complex assembly is made possible through the use of the type IIS restriction enzymes *BsaI* and *BpiI*. Unlike the more common type II restriction enzymes such as *HindIII*, type IIS enzymes cut DNA outside of the recognition site, as opposed to inside it (Szybalski *et al.*, 1991). This allows for the creation of tailored 4 bp overhangs known as fusion sites. These fusion sites act as puzzle pieces, only allowing modules with the correct sites to be added. As such, this allows for interchangeability of the modules, so long as they have the correct fusion sites. Different levels use different vector backbones containing the origin of replication, an antibiotic resistance gene and the *LacZ* gene. The antibiotic resistance gene is different at each level, spectinomycin at level 0, ampicillin at Level 1 and kanamycin at Level 2. This ensures that only the wanted construct is present when transitioning between levels. The presence of the *LacZ* gene is important as a selection marker, as it is replaced by the modules during the reaction. Consequently, when transformed into *E. coli* colonies with the modules inserted will appear white, while those without it will appear blue in the presence of IPTG as an inducer and X-Gal as a substrate that makes a blue chromophore when galactose sugar is removed.

***Nicotiana benthamiana* as a heterologous host**

Nicotiana benthamiana has been used in plant research for approaching half a century, carving out its niche in as a heterologous host due to its susceptibility to many viruses unable to infect *A. thaliana* due a mutation in *rdr1* (Quacquarelli and Avgelis, 1975)(Yang *et al.*, 2004). However, it has become more widely used as more sophisticated technologies were developed. Among these technologies is agroinfiltration, a technique used to express foreign proteins in the leaves of *N. benthamiana* (Schöb, Kunz and Meins, 1997). A

suspension of *Agrobacterium tumefaciens* cells transformed with plasmids designed to enable expression of a gene, often fluorescently tagged, is injected into the intracellular space within a leaf. After three days *A. tumefaciens* has transformed the infiltrated area of the leaf and the protein is expressed, enabling microscopy or biochemical analysis to be carried out. This simple method is flexible and enables the expression of multiple proteins in the same leaf at once, making it perfect for investigating protein-protein interactions. Additionally, each plant can support multiple transformations at once, is easy to care for and ready for infiltration within 3-4 weeks making a medium throughput feasible.

β-glucuronidase (GUS)

The β-glucuronidase (GUS) reporter system is one of the most popular molecular biology techniques in the world. Since its inception in 1987 (Jefferson, Kavanagh and Bevan, 1987) it has been used widely across the world in thousands of labs. The system utilises the GUS protein from *Escherichia coli*, an enzyme capable of hydrolysing the colourless 5-bromo-4-chloro-3-indolyl glucuronide substrate into the blue coloured 5,5'-dibromo-4,4'-dichloro-indigo (diX-indigo) compound. Here this ability has been leveraged for use as a reporter for the Level 2 constructs. By including a GUS module in the Level 2 construct containing the tagged CBL and CIPK proteins, it will be expressed in the leaf tissue alongside the proteins of interest. A simple GUS staining protocol will allow for the identification of failed transformations, as they will not turn blue, eliminating the possibility of false negatives.

3.1.3 Previous work and the next steps

Identifying CBL-CIPK interactions in *M. polymorpha*

This experiment is building upon and improving previous work in the Miller lab. Previously we have used a co-infiltration strategy, infiltrating *N. benthamiana* with a pair of Level 1 constructs which individually transform the plant material. This experiment indicated that all but the CIPK-A/CBL-C interaction occurred *in planta*. However, while this system did provide positive results, it was limited in repeats and crucially, was lacking a reporter. It could not be ruled out that this lacking interaction was not down to a failed transformation in one or both of the Level 1 constructs. As such this experiment moves to eliminate that possibility by mobilising the Level 1 constructs into Level 2, reducing the number of points of failure to one. Additionally, a GUS reporter module, will be included in the final constructs, allowing for visual confirmation of transformation via GUS staining, eliminating the possibility of assaying a failed transformation and producing a false negative.

Identifying to role of CIPK-B in salt stress signalling.

Following qRT-PCR data showing overall downregulation of *CIPK-B* in saline conditions, CIPK-B was identified as the most likely SOS2 homologue candidate in *M. polymorpha*. In order to validate this suspicion, CIPK-B knockout mutants *cipk-b-1* and *cipk-b-2* have been generated using CRISPR-Cas9. These knockout lines will be exposed to NaCl in concentrations up to 150 mM following phenotyping experiments in *A. thaliana* (Awlia *et al.*, 2016).

3.2 Identifying CBL-CIPK interactions in *M. polymorpha*

3.2.1 Cloning: Level 0 to Level 2

The required constructs

As stated previously, the work described here is a continuation of work performed as my undergraduate research project. As part of this project, many of the Level 1 plasmids used in this study had already been created. However, as AtCBL4 and AtCIPK24 were not previously used as a positive control, these needed generating, as did the GUS module required for confirmation of transformation. The required Level 0 constructs for AtCIPK24 and GUS were already present in the Miller lab, however AtCBL4 was not and as such required generating. Table 3.1 describes the required fragments for the generation of BM01267, the level 0 plasmid containing AtCBL4. Where listed, constructs prefaced with 'EC' were generated as part of the 2015 Patron *et al.*, paper (Patron et al., 2015). Constructs prefaced with BM have been generated in the Miller lab.

Table.3.1 Level 0 constructs. Cells shaded green indicate constructs or DNA generated as part of this study. Shells shaded red indicate constructs previously present in the Miller Lab.

ID	Backbone	S/SC1
BM01267	EC15456 pL0V-SC1	AtCBL4 PCR

Three Level 1 constructs were generated, constructs BM01167, BM01177 and BM01178. These construct IDs represent AtCIPK24 with a Small BiT fusion tag, AtCBL4 with a Large BiT fusion tag, and the GUS module. The composition of these constructs is displayed below in Table 3.2.

Table.3.2 Level 1 Constructs. Cells shaded green indicate constructs generated as part of this study. Shells shaded red indicate constructs previously present in the Miller Lab.

ID	Backbone	Promoter	S/SC1	C/C2	Terminator
BM01167	EC47822 pL1V-R3	EC15057 pNOS	BM00917 pL0M-S-SmBiT	BM01151 pL0M-C-AtCIPK24	EC41421 tNOS
BM01177	EC47802 pL1V-R1	EC15058 p35S(short)	BM01267 pL0M-SC1-AtCBL4	BM00916 pL0M-S-LgBiT	EC41414 t35S
BM01178	EC47811 pL1V-R2	EC15062 pAtUBI10	EC75111 - GUS	-	EC41421 tNOS

Twenty Level 2 constructs were generated, constructs BM01268 – BM01287. These Level 2 constructs all conform to the same basic structure, an CBL with a Small BiT fusion tag, a

GUS module for confirmation of transcription, and a CIPK with a Large BiT fusion tag. The composition of all of these constructs is displayed below in Table 3.3.

Table.3.3 Level 2 constructs. Cells shaded green indicate constructs generated as part of this study. Shells shaded yellow indicate constructs generated as part of my undergraduate project. Shells shaded red indicate constructs previously present in the Miller Lab

ID	Backbone	1	2	3	End Linker
BM01268	EC50505	BM01064 - MpCBL-A	BM01178	BM01067 - MpCIPK-A	EC41766
BM01269	EC50505	BM01065 - MpCBL-B	BM01178	BM01067 - MpCIPK-A	EC41766
BM01270	EC50505	BM01066 - MpCBL-C	BM01178	BM01067 - MpCIPK-A	EC41766
BM01271	EC50505	BM01177 - AtCBL4	BM01178	BM01067 - MpCIPK-A	EC41766
BM01272	EC50505	BM01064 - MpCBL-A	BM01178	BM01068 - MpCIPK-B	EC41766
BM01273	EC50505	BM01065 - MpCBL-B	BM01178	BM01068 - MpCIPK-B	EC41766
BM01274	EC50505	BM01066 - MpCBL-C	BM01178	BM01068 - MpCIPK-B	EC41766
BM01275	EC50505	BM01177 - AtCBL4	BM01178	BM01068 - MpCIPK-B	EC41766
BM01276	EC50505	BM01064 - MpCBL-A	BM01178	BM01069 - Δ NAF-MpCIPK-A	EC41766
BM01277	EC50505	BM01065 - MpCBL-B	BM01178	BM01069 - Δ NAF-MpCIPK-A	EC41766
BM01278	EC50505	BM01066 - MpCBL-C	BM01178	BM01069 - Δ NAF-MpCIPK-A	EC41766
BM01279	EC50505	BM01177 - AtCBL4	BM01178	BM01069 - Δ NAF-MpCIPK-A	EC41766
BM01280	EC50505	BM01064 - MpCBL-A	BM01178	BM01070 - Δ NAF-MpCIPK-B	EC41766
BM01281	EC50505	BM01065 - MpCBL-B	BM01178	BM01070 - Δ NAF-MpCIPK-B	EC41766
BM01282	EC50505	BM01066 - MpCBL-C	BM01178	BM01070 - Δ NAF-MpCIPK-B	EC41766
BM01283	EC50505	BM01177 - AtCBL4	BM01178	BM01070 - Δ NAF-MpCIPK-B	EC41766
BM01284	EC50505	BM01064 - MpCBL-A	BM01178	BM01167 - AtCIPK-24	EC41766
BM01285	EC50505	BM01065 - MpCBL-B	BM01178	BM01167 - AtCIPK-24	EC41766
BM01286	EC50505	BM01066 - MpCBL-C	BM01178	BM01167 - AtCIPK-24	EC41766
BM01287	EC50505	BM01177 - AtCBL4	BM01178	BM01167 - AtCIPK-24	EC41766

Constructs BM01276 – BM01282 use Δ NAF CIPKs in position 3, these are CIPKs from which the NAF domain has been removed. The work to do this and produce Level 0 constructs containing the requisite sequence was completed by Dr Connor Tansley. The NAF domain is the domain through which CBLs and CIPKs interact and is both required and sufficient for the binding of CBLs and CIPKs (Albrecht *et al.*, 2002). As such the removal of this domain prevents the binding of CBLs and CIPKs. These constructs will be used as a negative control to compare each individual CBL-CIPK pairing, as well as indicating that any observed luminescence is a result of a CBL-CIPK interaction, and not chance recombination of the NanoLuc luciferase.

To illustrate this process I will present the full lifecycle of the Level 0 AtCBL4 fragment, looking at Constructs BM01267, BM01177 and BM01271.

Level 0

To be able to use AtCBL4 in a construct, it requires sub-cloning to the correct position for use in the Golden Gate Cloning system. This includes the addition of the requisite *BpiI* restriction enzyme site, and the fusion tags for SC1 position, AATG and GGTG. This process was carried out using Phusion PCR using the primer pair C222/C223 (Appendix.1), amplifying cDNA of CBL4. The PCR product was visualised via gel electrophoresis and the expected 694 bp fragment seen in Fig.3.1A. As such the band was extracted and purified. This purified DNA was used in a Golden Gate reaction containing the EC15456 backbone and the Phusion PCR product, as per BM01267 in Table.3.1, transformed into *E. coli*. This generates a Level 0 plasmid as illustrated in Fig.3.1A, containing a spectinomycin resistance gene, and AtCBL4. As the AtCBL4 DNA has displaced the LacZ gene native to the EC15456 backbone, blue-white screening is possible. The transformation was plated on to LB-agar plates containing spectinomycin, and a selection of white colonies sampled for colony PCR using the C222/C223 primer pair. Colonies 1, 2, 3 and 6 were identified as positive. Colony1 was grown up overnight, DNA extracted and successfully sequenced both forwards and in reverse using C222 and C223 respectively.

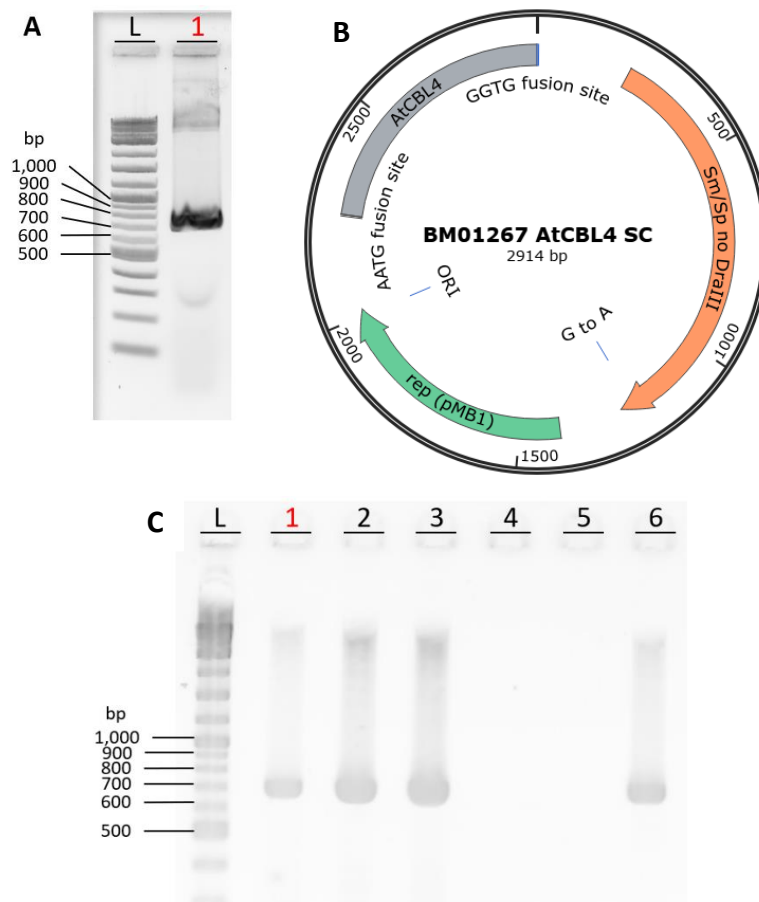


Figure 3.1 Successfully sub-cloning AtCBL4 into the Level 0 SC1 position (BM01267) A: PCR amplification of synthetic AtCBL4 cDNA. Lane L contains the 1kb+ ladder. Lane 1 contains the product resulting from a PCR reaction using AtCBL4 cDNA as a template, amplified with the primer pair C222/C223. A fragment of ~700 bp was generated. **B: A plasmid map of BM01267, generated using SnapGene software (www.snapgene.com).** **C: Colony PCR of BM01267.** Lane L contains the 1kb+ ladder. Lanes 1-6 contain colony PCR products of potential BM01267 colonies, amplified using the primer pair C222/C223, generating a PCR product of the expected ~700 bp.

Level 1

Now AtCBL4 has been cloned into the SC1 position, it can be used in a level 1 Golden Gate reaction to generate the NanoBiT tagged fusion protein. CBLs were tagged with the LargeBiT on the C-Terminus, CIPKs with the SmallBiT on the N-terminus. As a reporter, the GUS module was not made into a fusion protein. Full assembly of the Level 1 constructs can be found in Table.3.2. Following AtCBL4, a Golden Gate reaction was set up as per BM01177 in Table.3.2, the resultant plasmid can be seen in Fig.3.2A and contains an ampicillin resistance gene, and the desired AtCBL4-LargeBiT fusion protein. This plasmid was transformed into *E. coli* and plated on to LB agar plates containing ampicillin. A selection of white colonies were sampled for colony PCR using the C222/C223 primer pair, seen below in Fig.3.2B.

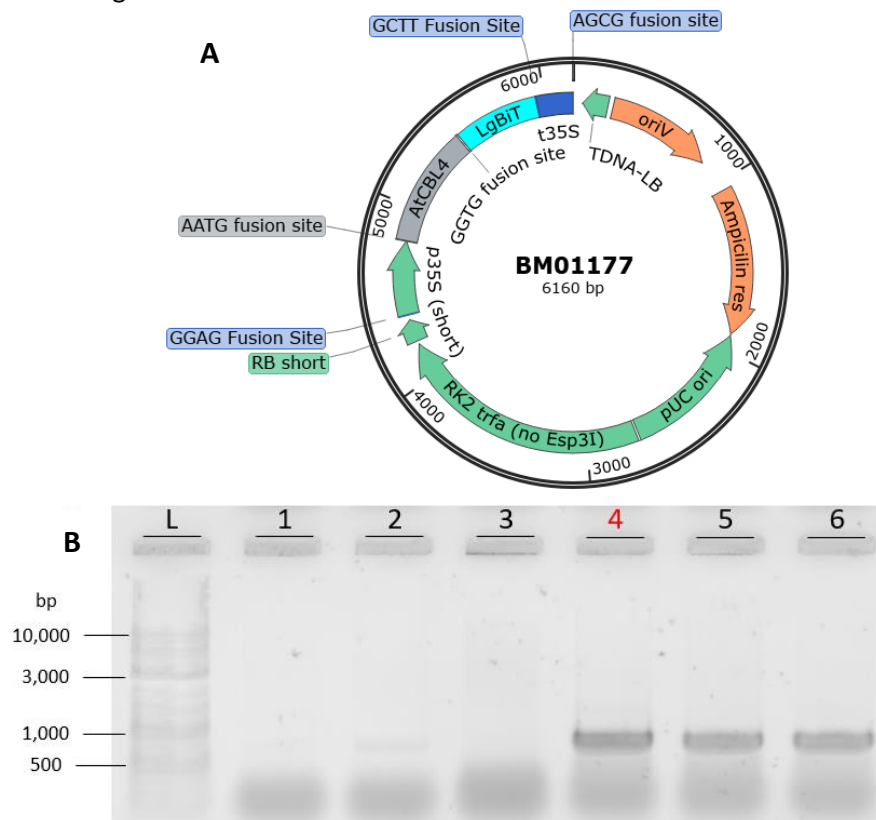


Figure 3.2 Successfully generation of the Level 1 construct BM01177. A: A plasmid map of BM01267, generated using SnapGene software (www.snapgene.com) B: Colony PCR of BM01177 Lane L contains the 1kb+ ladder. Lanes 1-6 contain colony PCR products of potential BM01177 colonies, amplified using the primer pair C222/C223. Colony (4) was picked and used in further experiments.

Colonies 1 and 3 were negative, colony 2 shows a faint positive, and colonies 4, 5 and 6 showed strong positives. Colony 4 was picked, grown up overnight and the DNA extracted. This DNA was successfully sequenced using the C222/C223 primer pair.

Level 2

With BM01177 and the other outstanding Level 1 constructs synthesised, generation of Level 2 constructs could begin. All Level 2 constructs were combined in the same way, the Level 1 CBL module in position 1, the GUS module in position 2 and the CIPK module in position 3. CIPK-A and CIPK-B were paired with CBL-A, CBL-B and CBL-C, as well as AtCBL4. Additionally, a Δ NAF CIPK negative control was made for each of these interactions. The positive control of AtCIPK24 and AtCBL4 was constructed, as well as pairing AtCIPK24 with each of the three *M. polymorpha* CBLs. These constructs are detailed in Table3.3. Following BM01177, it is paired with CIPK-A in BM01271, the Golden Gate reaction carried out as per BM01271 in Table3.3. The plasmid map of BM01271 is depicted in Fig.3.3A, containing a Kanamycin resistance gene, AtCBL4 tagged with LargeBiT, GUS, and MpCIPK-A tagged with SmallBiT. The result of the Golden Gate reaction was then transformed into *E. coli* and plated on to LB agar containing kanamycin. A selection of white colonies were sampled for colony PCR using the C222/C223 primer pair, seen below in Fig.3.3B. All three colonies were positive, showing a band at around 700 bp. Colony 1 was picked and grown overnight and the DNA extracted. This DNA was digested by *EcoRI* and visualised by gel electrophoresis, seen in Fig.3.3C. The appropriate banding pattern was seen and the DNA sequenced both forwards and in reverse using C222 and C223 respectively.

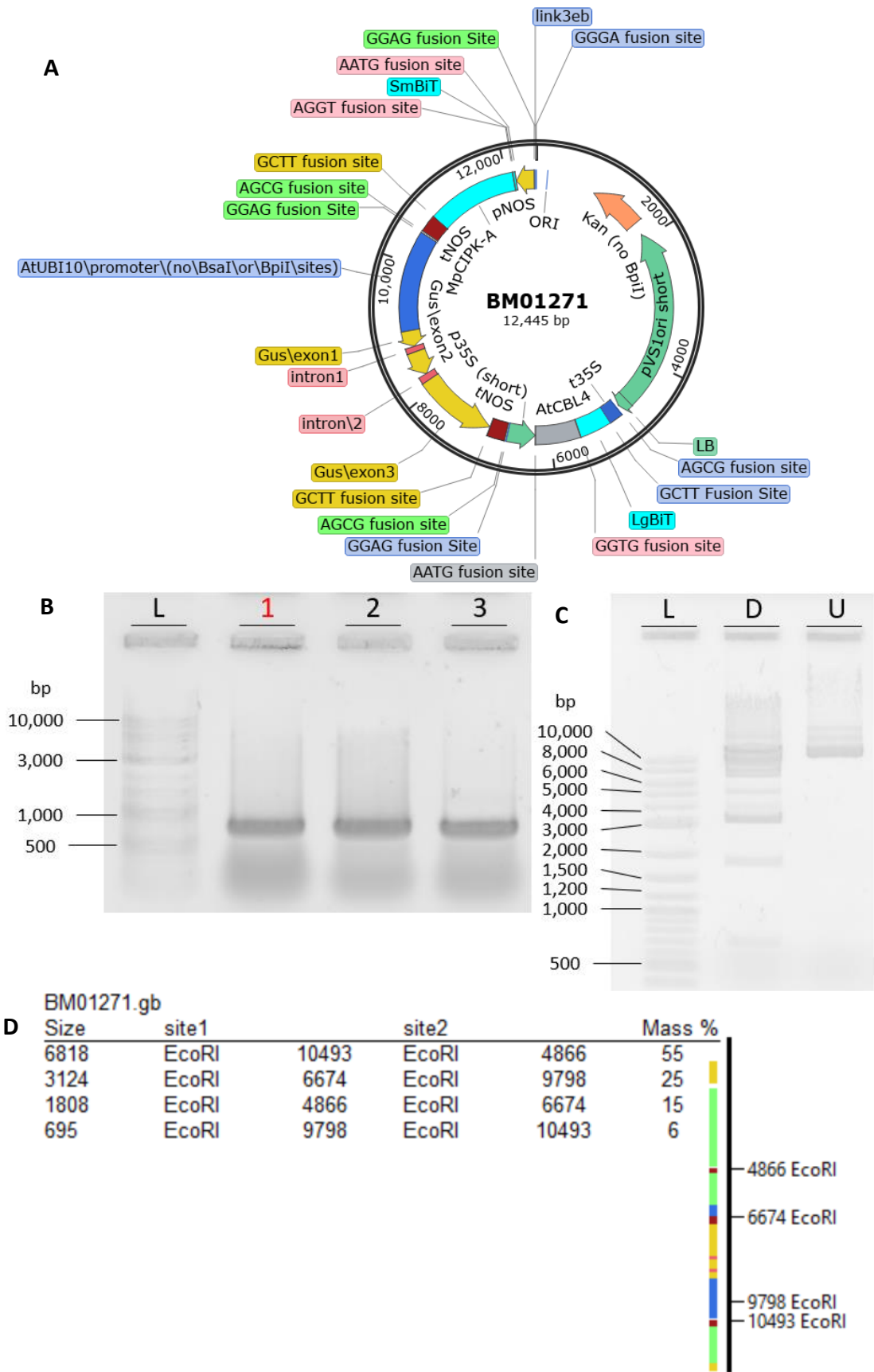


Figure 3.3 Successfully generation of the Level 2 construct BM01271. **A:** A plasmid map of BM01271, generated using SnapGene software (www.snapgene.com) **B:** Colony PCR of

BM01177. Lane L contains the 1kb+ ladder. Lanes 1-3 contain colony PCR products of potential BM01267 colonies, amplified using the primer pair C222/C223. Colony (1) was picked and used in further experiments. **C: Digestion of BM01177 by *EcoRI*,** Lane L contains the 1kb+ ladder. Lane D contains the BM01271 DNA digested with *EcoRI*, Lane U contains undigested BM01271 DNA. **D: Expected band sizes for digestion of BM01271 by *EcoRI*, generated using ApE** (Davis & Jorgensen, 2022)

All three colonies were positive, showing a band at around 700 bp. Colony 1 was picked and grown overnight and the DNA extracted. This DNA was digested by *EcoRI* and visualised by gel electrophoresis, seen in Fig.3.5C. Bands can be seen at the expected values of 695, 1,808, 3,124 and 6,818, however, there are also bands at approximately 4,000 and 5,000, as well as several between 6,000 and 12,000. These anomalies can be explained by incomplete digestion of the plasmid, or potential contamination by aberrant golden gate reactions, as multiple bands can be seen in the undigested lane. As this issue was persistent across multiple picked colonies, and different constructs, it was decided to proceed with this colony. An *EcoRI* digest of all Level 2 constructs was carried out as confirmation of their synthesis and has been included below in Fig.3.4A. Constructs in lanes 3, 7, 11, 15 and 19 all contain MpCBL-C, which contains an internal *EcoRI* restriction site. This changes the expected banding pattern to five bands, 695, 768, 1013, 3124 and 6818, as depicted in Fig.3.4B. Due to the two smallest bands being very close in size, it was not possible to completely resolve them, leading to them appearing as one larger band. All other constructs follow the banding pattern shown in Fig.3.3.D. While faint in some cases, all of the constructs do achieve the expected banding patterns. However, as seen previously, some do have additional banding, possibly caused by contamination of the DNA, or incomplete digestion. As previously this was a continuous issue and the decision was made to proceed with the constructs shown below.

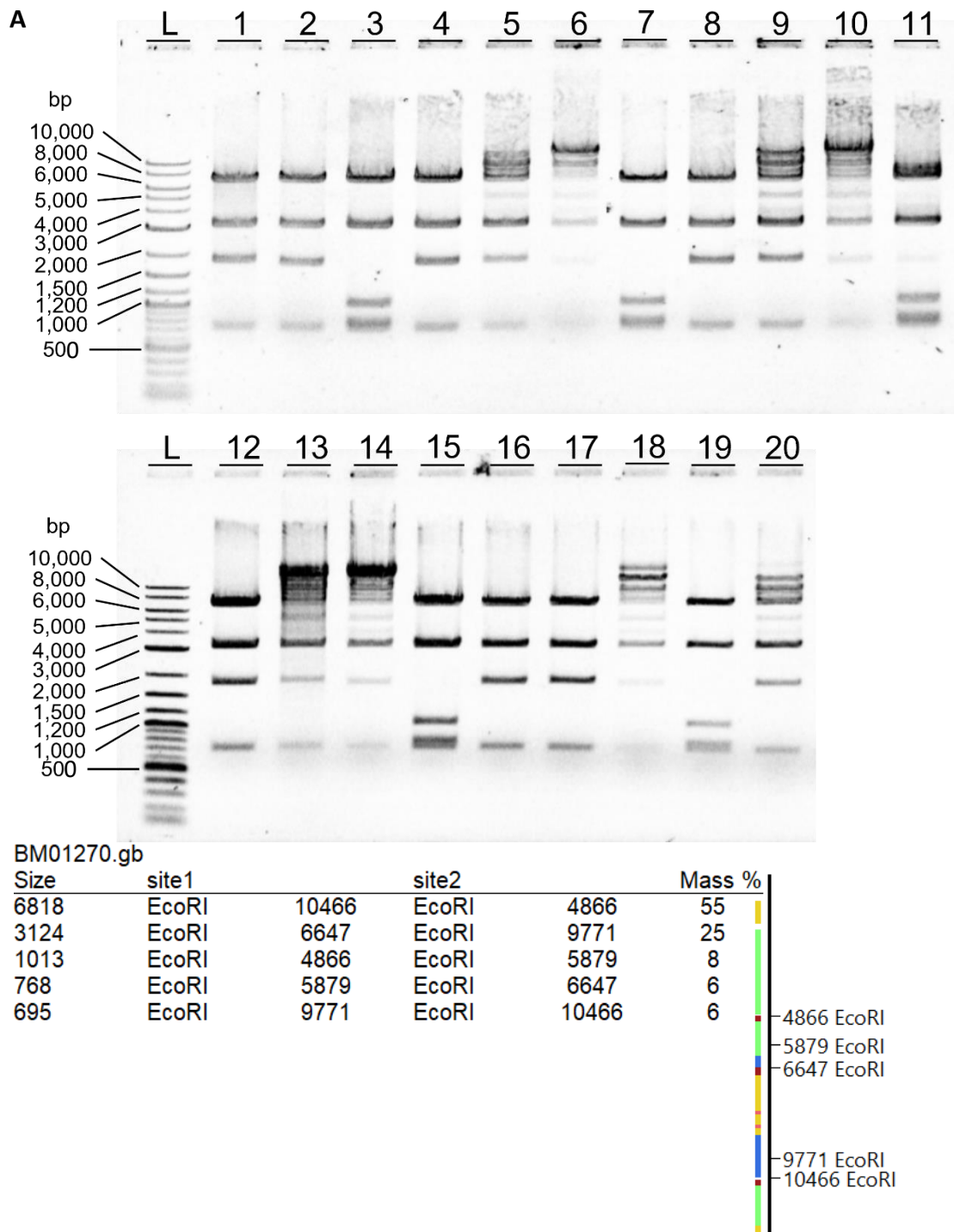


Figure.3.4 Level 2 constructs have been successfully generated A: 3.4 EcoRI digest of all synthesised level 2 constructs. Lanes L contain the 1kb+ ladder. Lanes 1-20 contain the EcoRI digested product of the synthesised Level 2 constructs, ordered as they appear in Table3.3 **B: D: Expected band sizes for digestion of BM0127o by EcoRI, generated using ApE** (Davis & Jorgensen, 2022). This banding pattern is indicative of all constructs containing MpCBL-C.

3.2.2 NanoBiT assay indicates there is no specificity in CBL-CIPK interactions in *Marchantia polymorpha*

NanoBiT assays and preparations.

All synthesised Level 2 constructs were transformed into *Agrobacterium tumefaciens*, plated onto Lb agar containing rifampicin, gentamycin and kanamycin and incubated for 3 days at 28°C. Once colonies had grown, one of each construct was selected and grown up overnight. These cultures were prepared for infiltration and infiltrated into *Nicotiana benthamiana* the next day, alongside an acetosyringone only control. The infiltrated plants were left at room temperature for three days, and plant material harvested. One leaf punch was taken and GUS stained to ensure the transformation was successful, another taken and flash frozen in liquid nitrogen. These leaves were then processed according to the Nano-Glo® Live Cell Assay System Protein assay and the results visualised on the Hidex sense microplate reader. This was performed in triplicate for both biological and technical replicates.

CBL-CIPK interactions in *M. polymorpha* appear to be non-specific

Once all assays had been conducted the data was pooled. Within each replicate the data was normalised to the acetosyringone control, providing a luminescence fold change in relation to the control. These results are presented below in Figure.3.5.

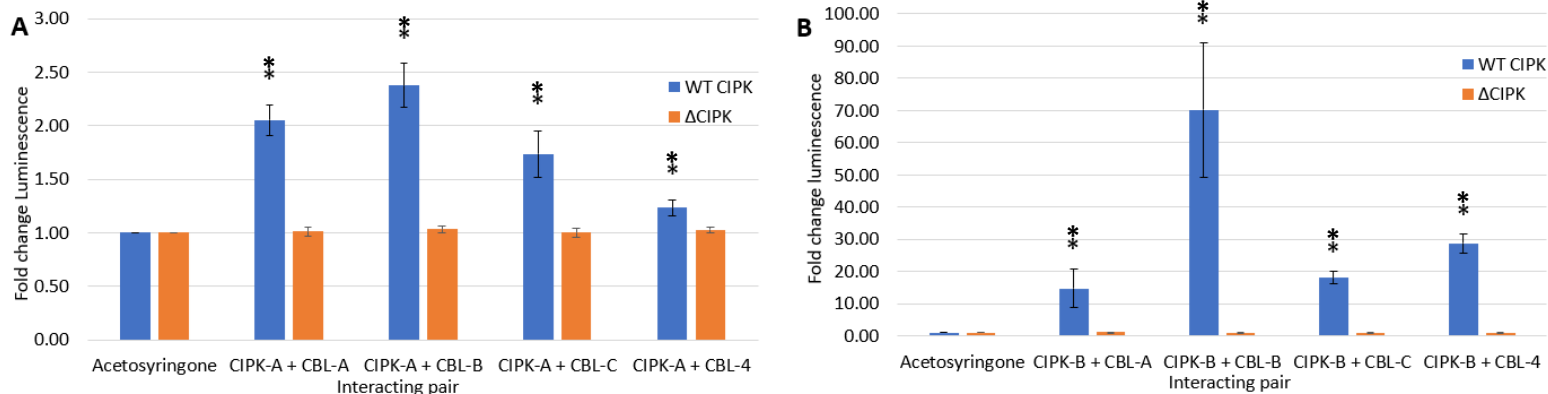


Figure.3.5. CBL-CIPK interactions in *M. polymorpha* appear to be non-specific. The data is expressed as a ratio of the acetosyringone control. Column labels show the interaction between two fusion proteins. Significance in a pairwise two-tailed *t*-test relative to the corresponding ΔNAF interacting pair is denoted: **, $P < 0.01$. Standard error is shown as error bars.

Both CIPK-A and CIPK-B appear to interact with all of the *M. polymorpha* CBLs, as well as AtCBL4. However the magnitude of these interactions appears to be very different. The Luminescence produced by CIPK-A interactions ranges between 1.23 and 2.38, compared

to the lowest of 14.73 and maximum of 70.17 produced by interactions with CIPK-B. This does not necessarily denote interaction strength, but could rather be explained by competition from CBLs present in *N. benthamiana*, sequestering CIPK-A and preventing binding. Another possibility is that the expression systems in *N. benthamiana* are less well optimised for the production of CIPK-A than CIPK-B, leading to a lower expression of CIPK-A perhaps caused by different codon preference between *N. benthamiana* and *M. polymorpha* (Atef *et al.*, 2020). Additionally, there maybe some element of steric hinderance to the system from the NanoBiT tags in CIPK-A that is not present in CIPK-B. As such these luminescence readings should only be taken as a proof of binding, not an allusion to its strength. To investigate the strength of interaction further, several avenues are available. Now knowing that all interactions are possible, a pulldown assay with purified proteins could be performed. This could be carried out by expressing the CIPK of interest with a protein tag such as a his-tag with a cleavage site that could then be extracted and pulled down from a nickel affinity column and cleaved from the column allowing for only the elution of the CIPK and any interacting partners (Spriesterbach *et al.*, 2015). Another option is performing a similar experiment in *M. polymorpha* by tagging native proteins with the same NanoBiT system. This has the benefit of occurring in the organism of interest, and as such there will be no interference from foreign proteins. Additionally this method would allow for the visualisation of real time responses, through tracking the luminescence at set time points when exposed to a stress. However, while immensely powerful, this would also be very challenging as the technology for genetically modifying *M. polymorpha* is limited. There has been success in the Miller lab Knocking out CIPK-B with CRISPR (Tansley *et al.*, 2022) however tagging the genes of interest would prove more difficult. This represents an intensive project and is likely out of reach until such a time the throughput of transformation improves.

CIPK24

With the aim of identifying a possible *M. polymorpha* homologue to AtCBL4, the interactions between AtCIPK24 and the *M. polymorpha* CBLs was tested. The data for these interactions is presented below in Figure.3.6.

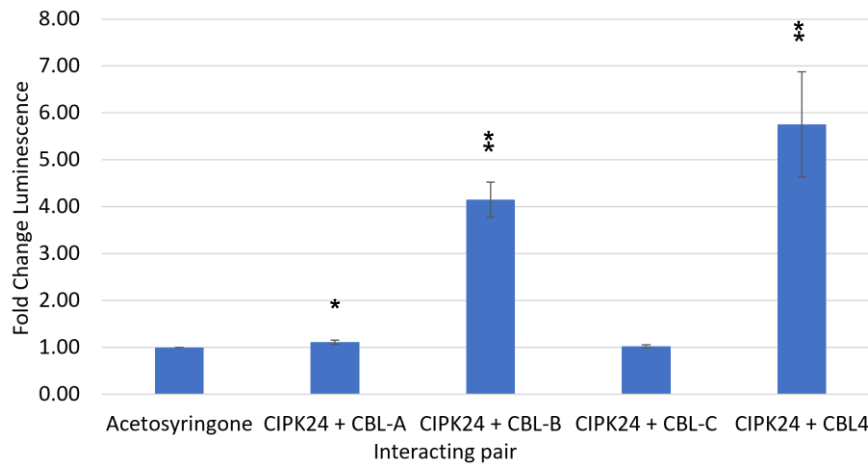


Figure.3.6. AtCIPK24 only interacts with MpCBL-B. The data is expressed as a ratio of the acetosyringone control. Column labels show the interaction between two fusion proteins. AtCIPK24 + AtCBL4 has been included as a positive control. Significance in a pairwise two-tailed *t*-test relative to the acetosyringone control is denoted: *, $P < 0.05$, **, $P < 0.01$. Standard error is shown as error bars.

AtCIPK24 was capable of binding MpCBL-A and MpCBL-B, but unable to bind CBL-C. This indicates that either MpCBL-A or MpCBL-B are candidates for a AtCBL4 homologue in *M. polymorpha*. As both CIPK-A and CIPK-B were capable of binding AtCBL4, yet AtCIPK24 was unable to bind all of the MpCBLs, this suggests the promiscuity shown is a function of the CIPKs and not the CBLs. To further test this possibility other AtCBLs could be integrated into this experiment to see how far this promiscuity extends.

3.3 CIPK-B is necessary for salt tolerance in *Marchantia polymorpha*

Following qRT-PCR data showing overall downregulation of *CIPK-B* in saline conditions, CIPK-B was identified as the most likely *SOS2* homologue candidate in *M. polymorpha*. In order to further investigate this, CIPK-B knockout mutants *cipk-b-1* and *cipk-b-2* were generated using CRISPR. The knockouts have been characterised as truncated proteins, generated by the early introduction of a stop codon, as can be seen in Fig.3.7.

	sgRNA1																sgRNA2																									
	G	GTC	GGT	CGT	ACC	ATT	GGC	G	G	GTC	AAG	TTC	GCC	CAG	AAC	A																										
<i>MpCIPK-B</i> 1	ATG	GTG	GTC	AGA	AAG	GTA	GGC	AAG	TAT	GAG	GTC	GGT	CCT	ACC	ATT	GGC	GAG	GGG	ACA	TTT	GCG	AAG	GTC	AAG	TTC	GCC	CAG	AAC	ACG	GAG	ACA	GGA	GAG	AGC	GTT	GCC	ATG	AAG	GTT	TTG	GAT	AAA
	M	V	V	R	K	V	G	K	Y	E	V	G	R	T	I	G	E	G	T	F	A	K	V	K	F	A	Q	N	T	E	T	G	E	S	V	A	M	K	V	L	D	K
<i>Mpcipk-b-1</i> 1	ATG	GTG	GTC	AGA	AAG	GTA	GGC	AAG	TAT	GAG	GTC	GGT	CCT	ACC	ATT	G	-----										AA	CAC	GGA	GAC	AGG	AGA	GAG	CGT	TGC	CAT	GAA	GGT	TTT	GGA	TAA	
	M	V	V	R	K	V	G	K	Y	E	V	G	R	T	I												E	H	G	D	R	R	E	R	C	H	E	G	F	G	.	
<i>Mpcipk-b-2</i> 1	ATG	GTG	GTC	AGA	AAG	GTA	GGC	AAG	TAT	GAG	GTC	GGT	CCT	ACC	---	GGC	GAG	GGG	ACA	TTT	GCG	AAG	GTC	AAG	TTC	GCC	CAT	---	CAC	GGA	GAC	AGG	AGA	GAG	CGT	TGC	CAT	GAA	GGT	TTT	GGA	TAA
	M	V	V	R	K	V	G	K	Y	E	V	G	R	T	.	G	E	G	T	F	A	K	V	K	F	A	H	.	H	G	D	R	R	E	R	C	H	E	G	F	G	.

Figure.3.7 Alignment of *Mpcipk-b* knockout mutant lines, and wildtype *MpCIPK-B*. The first 126 nucleotides of *MpCIPK-B*, and their corresponding amino acid, are shown on the first row, with the two 20-nucleotide sgRNAs, shown above in their positions. The resulting mutations to *MpCIPK-B* are shown on the next two rows. Nucleotide deletion events are depicted with a red dash (–), substitutions with red text. Amino acid differences are also depicted below the nucleotide code, changes depicted in red.

Here, these mutants have been used to carry out phenotyping under salt stress conditions to ascertain the role of *MpCIPK-B* in salt stress signalling in *M. polymorpha*. Five 3x3 mm tissue samples from the tip of the thallus were placed on plates containing 0, 50, 100 and 150 mM NaCl, and grown at long day conditions for seven days. Day seven photographs from the first replicate are shown below in Fig.3.8

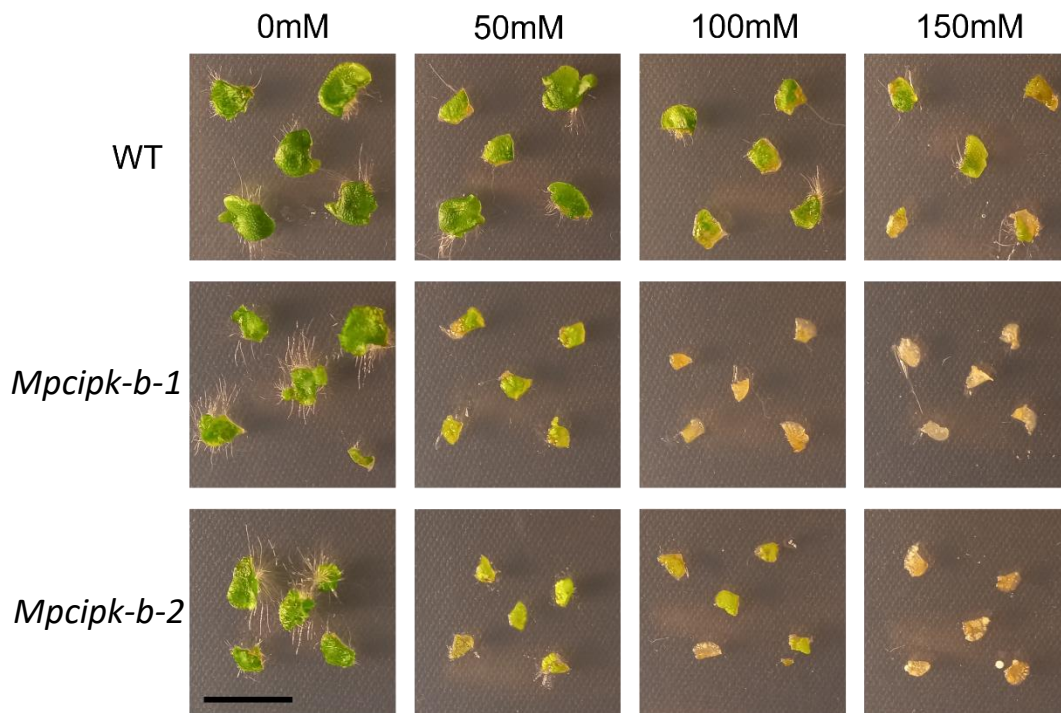


Figure.3.8. Salt sensitivity phenotyping. Images of day seven phenotyping. WT represents the CAM-2 wildtype control, 1247-1 and 1247-2 the two CIPK-B knockout mutants. Scale bar represents 1cm.

The WT sample exhibits a reduced growth phenotype, the size of the plants reducing as the concentration of NaCl in the media increases. The knockout mutants *cipk-b-1* and *cipk-b-2* exhibit a more extreme reduced growth phenotype, the plants appearing visibly smaller compared to their WT counterparts at each concentration. Additionally, the two mutant strains exhibit an additional phenotype of chlorosis in the higher concentrations of NaCl. This is only observed at 150mM in the WT sample, and to a reduced degree. To quantify

these observations, fresh weights were taken for all samples (Fig.3.9), and chlorophyll extraction and quantification (Fig.3.10) carried out.

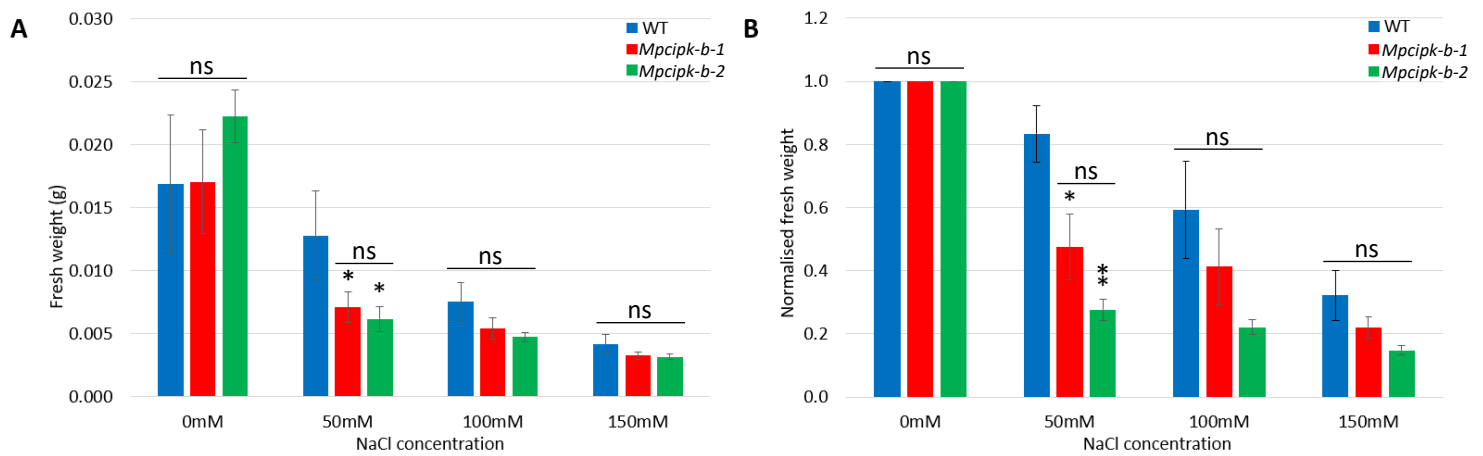


Figure 3.9. *cipk-b* mutants exhibit decreased growth. **A:** presents the raw data for the average pooled fresh weight. **B:** presents the normalised average pooled fresh weight data. Normalisation was carried out to the 0 mM values within each replicate. Significance in a Dunn's test, relative to the WT control is denoted: *, $P < 0.05$, **, $P < 0.01$. Standard error is shown as error bars

The fresh weight data presented in panel A supports the qualitative observations of the plant material. The measured fresh weights of the WT samples decrease as NaCl concentration increases, and the fresh weights of both mutant lines track closely together, below the WT readings. However, it is only at 50 mM is there significant difference between the mutants and the WT sample. The data in panel B has been normalised to the 0 mM value within each replicate, providing the average fold change in mass. This has the benefit of being able to take into account variances within each replicate, as well as to allow for better comparison between WT and mutant lines. When these variances are considered, the difference continues to be significant only at 50 mM, but at a higher level of confidence for *Mpcipk-b-2*. The statistical significance of these results indicate that the knockout of CIPK-B does indeed impair the ability of *M. polymorpha* to respond to salt stress, and as such is likely the SOS2 homologue. This is further reinforced by the chlorosis effect examined in Fig.3.12 below.

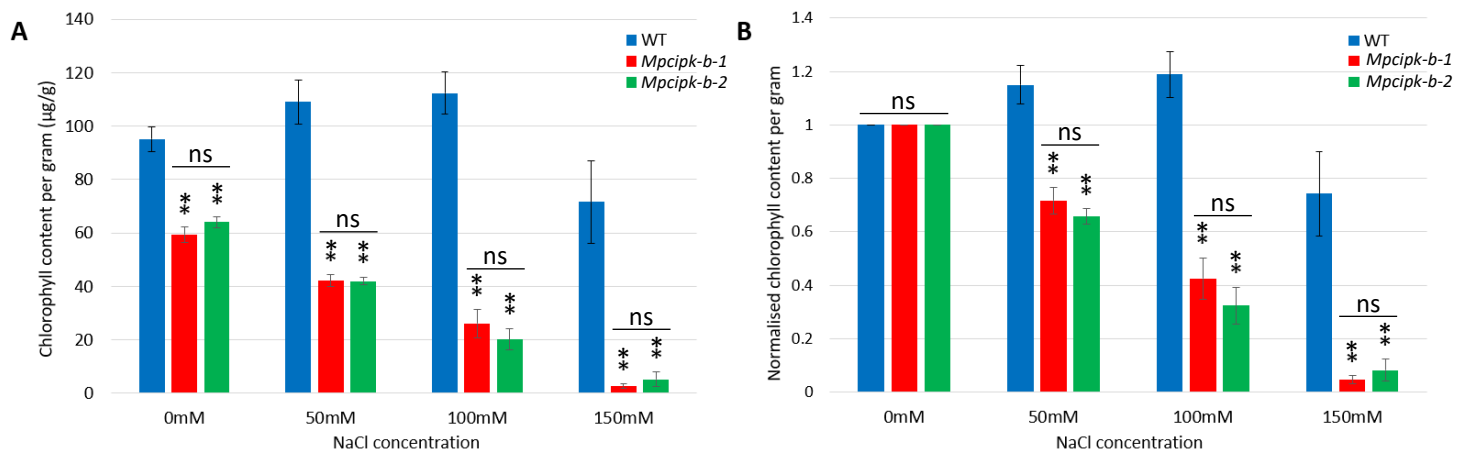


Figure.3.10. *Mpcipk-b* mutants exhibit increased levels chlorosis. **A:** presents the raw data for the average total chlorophyll content, per gram of each sample. **B:** presents the normalised average total chlorophyll content, per gram of each sample. Normalisation was carried out to the 0mM values within each replicate. Significance in a Dunn’s test, relative to the WT control is denoted: *, $P < 0.05$, **, $P < 0.01$. Standard error is shown as error bars.

Panel A of Fig.3.10 shows that even at the 0 mM control, the chlorophyll content per gram of the *Mpcipk-b* mutants is significantly lower than in the WT. This could be attributed to a number of factors including the developmental differences that have been observed in the mutant (Tansley *et al.*, 2022). There is an observable difference in the trend between the WT and the *Mpcipk-b* lines. Where the WT chlorophyll content of the WT line increases at 50 mM and 100 mM, though not statistically significantly so, only falling at 150 mM, the chlorophyll content of the *Mpcipk-b* lines decreases significantly from 50 mM NaCl. Despite the initial difference in chlorophyll content between *Mpcipk-b* lines and the WT, when normalising to the 0 mM control within each replicate, the statistical significance in the results remains. This statistical difference indicates that the chlorosis is brought about by the increasing salinity, and is not just a result of the differing physiology of the mutants.

4 Conclusion

To conclude, through the use of split luciferase assay using the novel NanoLuc luciferase, it has been illustrated that the CBLs and CIPKs of *M. polymorpha* bind non-specifically.

Additionally, while both MpCIPKs are capable of binding AtCBL4, AtCIPK24 was unable to bind MpCBL-C. This may indicate that the function for the polygamous nature of the CBL-CIPK interaction lies with the CIPKs of *M. polymorpha*, rather than shared characteristics between the MpCBLs. Now these interactions have been characterised, in order to better understand these interactions, a pulldown assay with HIS-tagged purified proteins could be performed. Another option would be to express NanoBiT tagged proteins *in planta*. This would allow for a number of investigations to be carried out, including identifying the localisation of the interacting pair (Waadt et al., 2008). An additional benefit of this system would be the ability to investigate binding under various stress conditions, however, at the present time CRISPR/CAS9 technology in *M. polymorpha* is not efficient enough to make production of the required lines feasible.

MpCIPK-B has been identified as being required for salt tolerance in *M. polymorpha*.

Mpcipk-b lines were more severely impacted by saline conditions, their growth being inhibited by a statistically significant 60% at 50 mM NaCl, when compared to a statistically insignificant 20% for wild type. Additionally mutant lines experienced much higher rates of chlorosis at all concentrations, with complete bleaching seen at 150 mM NaCl. Future work in this area should concentrate on generating the remaining knockouts for MpCIPK-A, and the three MpCBLs, allowing for investigation into the stress response roles of these proteins.

A Appendix

Appendix.1 List of primers used

Code	Target	Orientation	Sequence
C108	CBL-A	Forward	AGCGGAAAGAGGTGAAACGG
C109	CBL-A	Reverse	GAGAGGGATGCTGCTGAACC
C112	CBL-B	Forward	GGGCTGCTTCAGCTCAAAAC
C113	CBL-B	Reverse	CGCAAGCTGGAACTCTTCCT
C116	CBL-C	Forward	CAAGTGCTCCACCAGAGGAC
C117	CBL-C	Reverse	GCCTCCGCAAATGTCTTGTC
C120	CIPK-A	Forward	AAACACCCTGCGAACGAGAT
C121	CIPK-A	Reverse	ACCTCAAACACCTCTGTGGC
C126	CIPK-B	Forward	CCTCTCCGTTGCTATCGAGG
C127	CIPK-B	Reverse	ATTTCTGGCCTCTGCTTCGG
C204	AtCIPK24	Forward	tgtgaagaccaAGGTACAAAGAAAATGAGAAG
C205	AtCIPK24	Reverse	tgtgaagaccaAAGCTCAAACCGTGATTGTTC
C222	AtCBL4	Forward	tgtgaagaccaaattgGGCTGCTCTGTATCG
C223	AtCBL4	Reverse	tgtgaagacaacaccGGAAGATACGTTTTG
M52	GUS	Forward	GAATCCATCAGCGTAATG
M55	GUS	Reverse	CGACAGCAGCAGTTTCATC

B Bibliography

- Atef, A. *et al.*, 2020 Modification of paraburkholderia tale-like protein to activate transcription of target genes in plant, *Biosciences Biotechnology Research Asia*, 17(2), pp. 341–351.
- Albrecht, V., Ritz, O., Linder, S., Harter, K. and Kudla, J., 2001. The NAF domain defines a novel protein-protein interaction module conserved in Ca²⁺-regulated kinases. *The EMBO Journal*, 20(5), pp.1051-1063.
- Awlia, M., Nigro, A., Fajkus, J., Schmoeckel, S., Negrão, S., Santelia, D., Trtílek, M., Tester, M., Julkowska, M. and Panzarová, K., 2016. High-Throughput Non-destructive Phenotyping of Traits that Contribute to Salinity Tolerance in *Arabidopsis thaliana*. *Frontiers in Plant Science*, 7.
- Batistič, O., Waadt, R., Steinhorst, L., Held, K. and Kudla, J., 2009. CBL-mediated targeting of CIPKs facilitates the decoding of calcium signals emanating from distinct cellular stores. *The Plant Journal*, 61(2), pp.211-222.
- Bender, K., Zielinski, R. and Huber, S., 2018. Revisiting paradigms of Ca²⁺ signaling protein kinase regulation in plants. *Biochemical Journal*, 475(1), pp.207-223.
- Berridge, M., Lipp, P. and Bootman, M., 2000. The versatility and universality of calcium signalling. *Nature Reviews Molecular Cell Biology*, 1(1), pp.11-21.
- Bowman, J.L., Kohchi, T., Yamato, K.T., Jenkins, J., Shu, S., Ishizaki, K., Yamaoka, S., Nishihama, R., Nakamura, Y., Berger, F. and Adam, C., 2017. Insights into land plant evolution garnered from the *Marchantia polymorpha* genome. *Cell*, 171(2), pp.287-304.
- Braam, J., Sistrunk, M., Polisensky, D., Xu, W., Purugganan, M., Antosiewicz, D., Campbell, P. and Johnson, K., 1996. Life in a changing world: TCH gene regulation of expression and responses to environmental signals. *Physiologia Plantarum*, 98(4), pp.909-916.
- Bush, D., 1995. Calcium Regulation in Plant Cells and its Role in Signaling. *Annual Review of Plant Physiology and Plant Molecular Biology*, 46(1), pp.95-122.
- Caesar, J., Tamm, A., Ruckteschler, N., Leifke, A. and Weber, B., 2018. Revisiting chlorophyll extraction methods in biological soil crusts – methodology for determination of chlorophyll *a* and chlorophyll *a + b* as compared to previous methods. *Biogeosciences*, 15(5), pp.1415-1424.
- Chaves-Sanjuan, A., Sanchez-Barrena, M., Gonzalez-Rubio, J., Moreno, M., Ragel, P., Jimenez, M., Pardo, J., Martinez-Ripoll, M., Quintero, F. and Albert, A., 2014. Structural basis of the regulatory mechanism of the plant CIPK family of protein kinases controlling ion homeostasis and abiotic stress. *Proceedings of the National Academy of Sciences*, 111(42).
- Cheng, S., Willmann, M., Chen, H. and Sheen, J., 2002. Calcium Signaling through Protein Kinases. The *Arabidopsis* Calcium-Dependent Protein Kinase Gene Family. *Plant Physiology*, 129(2), pp.469-485.
- de Wet, J., Wood, K., Helinski, D. and DeLuca, M., 1985. Cloning of firefly luciferase cDNA and the expression of active luciferase in *Escherichia coli*. *Proceedings of the National Academy of Sciences*, 82(23), pp.7870-7873.

- Dixon, A., Schwinn, M., Hall, M., Zimmerman, K., Otto, P., Lubben, T., Butler, B., Binkowski, B., Machleidt, T., Kirkland, T., Wood, M., Eggers, C., Encell, L. and Wood, K., 2015. NanoLuc Complementation Reporter Optimized for Accurate Measurement of Protein Interactions in Cells. *ACS Chemical Biology*, 11(2), pp.400-408.
- Edel, K. and Kudla, J., 2015. Increasing complexity and versatility: How the calcium signaling toolkit was shaped during plant land colonization. *Cell Calcium*, 57(3), pp.231-246.
- Ehrhardt, D., Wais, R. and Long, S., 1996. Calcium Spiking in Plant Root Hairs Responding to Rhizobium Nodulation Signals. *Cell*, 85(5), pp.673-681.
- Engler, C., Kandzia, R. and Marillonnet, S., 2008. A One Pot, One Step, Precision Cloning Method with High Throughput Capability. *PLoS ONE*, 3(11), p.e3647.
- Hall, M., Unch, J., Binkowski, B., Valley, M., Butler, B., Wood, M., Otto, P., Zimmerman, K., Vidugiris, G., Machleidt, T., Robers, M., Benink, H., Eggers, C., Slater, M., Meisenheimer, P., Klaubert, D., Fan, F., Encell, L. and Wood, K., 2012. Engineered Luciferase Reporter from a Deep Sea Shrimp Utilizing a Novel Imidazopyrazinone Substrate. *ACS Chemical Biology*, 7(11), pp.1848-1857.
- Hussain, S., Hussain, S., Qadir, T., Khaliq, A., Ashraf, U., Parveen, A., Saqib, M. and Rafiq, M., 2019. Drought stress in plants: An overview on implications, tolerance mechanisms and agronomic mitigation strategies. *Plant Science Today*, 6(4), pp.389-402.
- Ishitani, M., Liu, J., Halfter, U., Kim, C., Shi, W. and Zhu, J., 2000. SOS3 Function in Plant Salt Tolerance Requires N-Myristoylation and Calcium Binding. *The Plant Cell*, 12(9), p.1667.
- Jamil, A., Riaz, S., Ashraf, M. and Foolad, M., 2011. Gene Expression Profiling of Plants under Salt Stress. *Critical Reviews in Plant Sciences*, 30(5), pp.435-458.
- Jefferson, R., Kavanagh, T. and Bevan, M., 1987. GUS fusions: beta-glucuronidase as a sensitive and versatile gene fusion marker in higher plants. *The EMBO Journal*, 6(13), pp.3901-3907.
- Knight, H., Trewavas, A. and Knight, M., 1997. Calcium signalling in Arabidopsis thaliana responding to drought and salinity. *The Plant Journal*, 12(5), pp.1067-1078.
- Kolkisaoglu, U., Weinl, S., Blazevic, D., Batistic, O. and Kudla, J., 2004. Calcium Sensors and Their Interacting Protein Kinases: Genomics of the Arabidopsis and Rice CBL-CIPK Signaling Networks. *Plant Physiology*, 134(1), pp.43-58.
- Kudla, J., Xu, Q., Harter, K., Gruissem, W. and Luan, S., 1999. Genes for calcineurin B-like proteins in Arabidopsis are differentially regulated by stress signals. *Proceedings of the National Academy of Sciences*, 96(8), pp.4718-4723.
- Li, W., Halling, D., Hall, A. and Aldrich, R., 2009. EF hands at the N-lobe of calmodulin are required for both SK channel gating and stable SK-calmodulin interaction. *Journal of General Physiology*, 134(4), pp.281-293.
- Liu, J. and Zhu, J., 1998. A Calcium Sensor Homolog Required for Plant Salt Tolerance. *Science*, 280(5371), pp.1943-1945.
- Mao, J., Manik, S., Shi, S., Chao, J., Jin, Y., Wang, Q. and Liu, H., 2016. Mechanisms and Physiological Roles of the CBL-CIPK Networking System in Arabidopsis thaliana. *Genes*, 7(9), p.62.
- Matthews, J., Hori, K. and Cormier, M., 1977. Purification and properties of Renilla reniformis luciferase. *Biochemistry*, 16(1), pp.85-91.

Kerppola, T.K., 2008 Bimolecular fluorescence complementation (BIFC) analysis as a probe of protein interactions in living cells, *Annual Review of Biophysics*, 37(1), pp. 465–487.

Mukherjee, S., Mishra, A. and Trenberth, K., 2018. Climate Change and Drought: a Perspective on Drought Indices. *Current Climate Change Reports*, 4(2), pp.145-163.

Nelson, M., Thulin, E., Fagan, P., Forsén, S. and Chazin, W., 2009. The EF-hand domain: A globally cooperative structural unit. *Protein Science*, 11(2), pp.198-205.

Nhieu, G., Clair, C., Grompone, G. and Sansonetti, P., 2004. Calcium signalling during cell interactions with bacterial pathogens. *Biology of the Cell*, 96(1), pp.93-101.

Patron NJ, Orzaez D, Marillonnet S, Warzecha H, Matthewman C, Youles M, Raitskin O, Leveau A, Farré G, Rogers C, Smith A, Hibberd J, Webb AA, Locke J, Schornack S, Ajioka J, Baulcombe DC, Zipfel C, Kamoun S, Jones JD, Kuhn H, Robatzek S, Van Esse HP, Sanders D, Oldroyd G, Martin C, Field R, O'Connor S, Fox S, Wulff B, Miller B, Breakspear A, Radhakrishnan G, Delaux PM, Loqué D, Granell A, Tissier A, Shih P, Brutnell TP, Quick WP, Rischer H, Fraser PD, Aharoni A, Raines C, South PF, Ané JM, Hamberger BR, Langdale J, Stougaard J, Bouwmeester H, Udvardi M, Murray JA, Ntoukakis V, Schäfer P, Denby K, Edwards KJ, Osbourn A, Haseloff J., 2015. Standards for plant synthetic biology: A common syntax for exchange of DNA parts. *New Phytologist*, 208(1), 13-19.

Qiu, Q., Guo, Y., Dietrich, M., Schumaker, K. and Zhu, J., 2002. Regulation of SOS1, a plasma membrane Na⁺/H⁺ exchanger in *Arabidopsis thaliana*, by SOS2 and SOS3. *Proceedings of the National Academy of Sciences*, 99(12), pp.8436-8441.

Quacquarelli, A. and Avgelis, A., 1975. *Nicotiana benthamiana* Domin, as host for plant viruses / *Nicotiana benthamiana* Domin, quale ospite di virus vegetali. *Phytopathologia Mediterranea*, 14(1), p.4.

Sánchez-Barrena, M., Fujii, H., Angulo, I., Martínez-Ripoll, M., Zhu, J. and Albert, A., 2007. The Structure of the C-Terminal Domain of the Protein Kinase AtSOS2 Bound to the Calcium Sensor AtSOS3. *Molecular Cell*, 26(3), pp.427-435.

Sánchez-Barrena, M., Martínez-Ripoll, M. and Albert, A., 2013. Structural Biology of a Major Signaling Network that Regulates Plant Abiotic Stress: The CBL-CIPK Mediated Pathway. *International Journal of Molecular Sciences*, 14(3), pp.5734-5749.

Sánchez-Barrena, M., Martínez-Ripoll, M., Zhu, J. and Albert, A., 2005. The Structure of the *Arabidopsis thaliana* SOS3: Molecular Mechanism of Sensing Calcium for Salt Stress Response. *Journal of Molecular Biology*, 345(5), pp.1253-1264.

Schöb, H., Kunz, C. and Meins, F., 1997. Silencing of transgenes introduced into leaves by agroinfiltration: a simple, rapid method for investigating sequence requirements for gene silencing. *Molecular and General Genetics MGG*, 256(5), pp.581-585.

Sedbrook, J., Kronebusch, P., Borisy, G., Trewavas, A. and Masson, P., 1996. Transgenic aequorin Reveals Organ-Specific Cytosolic Ca²⁺ Responses to Anoxia in *Arabidopsis thaliana* Seedlings. *Plant Physiology*, 111(1), pp.243-257.

Shi, H., Quintero, F., Pardo, J. and Zhu, J., 2002. The Putative Plasma Membrane Na⁺/H⁺ Antiporter SOS1 Controls Long-Distance Na⁺ Transport in Plants. *The Plant Cell*, 14(2), pp.465-477.

Shi, H., Quintero, F., Pardo, J. and Zhu, J., 2002. The Putative Plasma Membrane Na⁺/H⁺ Antiporter SOS1 Controls Long-Distance Na⁺ Transport in Plants. *The Plant Cell*, 14(2), pp.465-477.

Staxén, I., Pical, C., Montgomery, L., Gray, J., Hetherington, A. and McAinsh, M., 1999. Abscisic acid induces oscillations in guard-cell cytosolic free calcium that involve phosphoinositide-specific phospholipase C. *Proceedings of the National Academy of Sciences*, 96(4), pp.1779-1784.

Szybalski, W., C. Kim, S., Hasan, N. and J. Podhajski, A., 1991. Class-II restriction enzymes- a review. *Gene*, 109(1), p.169.

Tansley, C., Houghton, J., Rose, A.M.E, Witek, B., Payet, R., Wu, T. and Miller, J.B. 2022. CIPK-B is essential for salt stress signalling in *Marchantia polymorpha*. bioRxiv doi: 10.1101/2022.08.22.504506

Tracy F. E., Gilliham M., Dodd A. N., Webb A. A., Tester M. 2008. NaCl-induced changes in cytosolic free Ca²⁺ in *Arabidopsis thaliana* are heterogeneous and modified by external ionic composition. *Plant, Cell & Environment*, 31(8), pp.1063-1073.

Waadt R, Schmidt LK, Lohse M, Hashimoto K, Bock R, Kudla J. 2008. Multicolor bimolecular fluorescence complementation reveals simultaneous formation of alternative CBL/CIPK complexes in planta. *The Plant Journal* 56: 505–516.

Wayman, G., Tokumitsu, H., Davare, M. and Soderling, T., 2011. Analysis of CaM-kinase signaling in cells. *Cell Calcium*, 50(1), pp.1-8.

Weber, E., Engler, C., Gruetzner, R., Werner, S. and Marillonnet, S., 2011. A Modular Cloning System for Standardized Assembly of Multigene Constructs. *PLoS ONE*, 6(2), p.e16765.

Yang, S.-J. *et al.*, 2004. A natural variant of a host RNA-dependent RNA polymerase is associated with increased susceptibility to viruses by *nicotiana benthamiana*. *Proceedings of the National Academy of Sciences*, 101(16), pp. 6297–6302.